Ore Geology Reviews 130 (2021) 103947

Contents lists available at ScienceDirect

Ore Geology Reviews

journal homepage: www.elsevier.com/locate/oregeorev

Platinum mineralization and geochemistry of the Matysken zoned Ural-Alaskan type complex and related placer (Far East Russia)

Anton V. Kutyrev [a,*], Evgeniy G. Sidorov [a], Vadim S. Kamenetsky [a,b], Valery M. Chubarov [a], Ivan F. Chayka [b,c], Adam Abersteiner [d]

[a] Institute of Volcanology and Seismology, Far Eastern Branch of the Russian Academy of Sciences, Petropavlovsk-Kamchatsky, Russia
[b] Korzhinskii Institute of Experimental Mineralogy, Russian Academy of Sciences, Chernogolovka 142432, Russia
[c] V.S. Sobolev Institute of Geology and Mineralogy Siberian Branch of the Russian Academy of Sciences, Novosibirsk 630090, Russia
[d] Department of Geosciences and Geography (GeoHel), University of Helsinki, PO Box 64, FIN-00014 Helsinki, Finland

ARTICLE INFO

Keywords:
Platinum-group minerals
Dunite
Placer
Ural-Alaskan
Serpentine
Chromitite

ABSTRACT

Ural-Alaskan type complexes are the sources for unique placer platinum deposits and contain platinum-group minerals (PGM) within lodes. Such complexes occur along modern and ancient convergent tectonic margins and are comprised of dunite, wehrlite, clinopyroxenite and gabbro, which gradually interchange towards the marginal parts of the complex. In-situ PGM are largely restricted to chromitites, which are comprised of small veinlets and schlieren of chromian spinel in the dunite unit. PGM mineralization in chromitites can be extremely rich; however, their distribution is very sporadic, without any apparent regularity. Moreover, the role of accessory chromian spinel and post-magmatic overprinting of platinum group element (PGE) concentrations is poorly defined. Detailed studies of PGM assemblages, including those in chromitites, serpentine veinlets in dunites, and wehrlites, combined with PGE geochemistry could provide insights into the distribution and processes responsible for PGE accumulation.

The Matysken complex in the Koryak Highlands (Far East Russia) is comprised of dunite, wehrlite, clinopyroxenite and gabbro units, and has a classic zoned structure, rendering it an excellent example of an Ural-Alaskan type complex, ideal for this case study. This locality contains mm-scale isoferroplatinum (Pt_3Fe) nuggets that cement chromitites and occur as μm-scale euhedral inclusions in chromian spinel. Placer PGM assemblages in the nearby Matysken River consist of exactly the same assemblages of minerals that are found in dunites and chromitites but with larger compositional scatter, reflecting a complex history of alluvium accumulation, which was sourced from different eroded parts of the complex. Detailed textural investigations discovered a diverse array of hydrous silicate–related mineralization, including euhedral isoferroplatinum grains in chlorite matrix, isoferroplatinum–amphibole intergrowths, and a wide range of PGE, Fe and Cu alloys, sulfarsenides and antimonides, which formed in serpentine veinlets together with awaruite (Ni_3Fe) and base metal sulfides. This provides further evidence that isoferroplatinum, which is widely accepted to be a magmatic mineral, may form under a wide range of conditions, including during serpentinization.

Dunites have fractioned primitive mantle-normalized PGE patterns, typical of Ural-Alaskan type complexes, with strong enrichments in Pt and depletions in Ir, Ru and Pd. PGE, with an exception of Pd, are quite uniformly distributed in dunite containing accessory chromian spinel, with good correlations between PGE and Cr. This correlation, together with data from previous studies, allowed us to calculate the concentration of Pt in accessory chromian spinel (probably hosted as minute PGM inclusions), which is of the same grade as for chromitites (ppm levels). This suggests that the formation of chromitites does not concentrate PGE over Cr, but only assembles them into larger aggregates, causing the observed unevenness in the PGM distribution.

* Corresponding author.
E-mail address: anton.v.kutyrev@gmail.com (A.V. Kutyrev).

https://doi.org/10.1016/j.oregeorev.2020.103947
Received 24 August 2020; Received in revised form 12 December 2020; Accepted 16 December 2020
Available online 9 January 2021

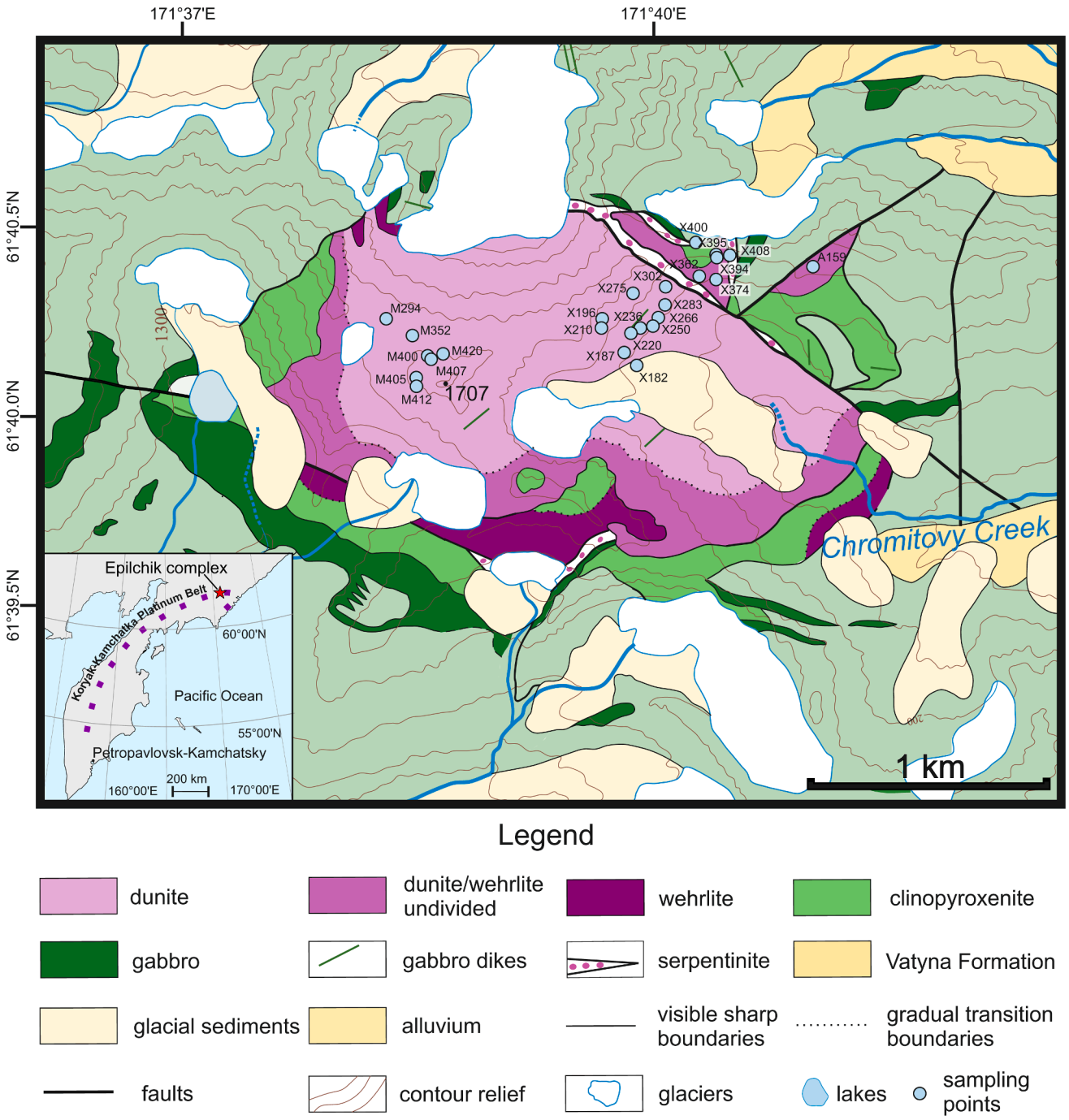

Fig. 1. Geological scheme of the Matysken Complex, modified after A. V. Razumny unpublished data (2000), and (Batanova and Astrakhantsev, 1992).

1. Introduction

The majority of platiniferous placer deposits are related to various ophiolitic ultramafics and Ural-Alaskan type zoned mafic–ultramafic complexes. The first are of low economic significance and have a prevailing amount of Ru-Ir-Os minerals, whereas the second may be large (up to hundreds of tons) and contain Pt-rich minerals with only subordinate amounts of other metals (Tolstykh et al., 2002a). Ural-Alaskan type complexes are defined by their zonal structure, petrographic composition (dunite, wehrlite, clinopyroxenite and gabbro) and their distribution along both modern and ancient convergent tectonic margins. They were first documented in the Uralian Platinum Belt of Russia (Loewinson-Lessing, 1900; Vysotsky, 1913) and later found in Alaska (Taylor, 1967), the Koryak-Kamchatka Platinum Belt in the Russian Far East (Batanova and Astrakhantsev, 1992; Batanova et al., 1991; Kutyev et al., 1991), British Colombia (Nixon et al., 1990), Colombia (Mertie, 1969), Venezuela (Murray, 1972), China (Qin et al., 2018; Cui et al., 2020) and numerous other regions worldwide. Previous studies demonstrated that the main repositories of Pt mineralization are chromitites – small veins and schlieren of chromian spinel, located within the central dunitic core of mafic–ultramafic complexes (Betekhtin, 1954; Ivanov, 1997; Johan, 2002; O'Driscoll and González-Jiménez, 2016; Tolstykh et al., 2015).

The presence of large placers and platinum mineralization in chromitites would make one to expect to find lode Pt deposits in Ural-Alaskan type complexes. Indeed, several attempts to estimate the value of lode chromitite-related Pt ores in Ural-Alaskan type complexes of the Ural Mountains and Koryak Highlands were conducted during the

20th and 21st centuries (Kozlov et al., 2011; Nazimova et al., 2011; Pushkarev et al., 2007; Razin, 1976; Stepanov et al., 2017). However, only the small but extremely high-grade Gosschakhta deposit in the Urals was mined at the beginning of the previous century. One of the main factors hindering exploration work is the extremely uneven distribution of PGM in dunite (Nazimova et al., 2011). Firstly, the distribution of chromitites themselves in the dunite core is extremely uneven, making standard sampling (0.5–1.5 kg) and drilling with standard core diameter ineffective (Nazimova et al., 2011; Sidorov et al., 2012). Similarly, the distribution of platinum-group minerals (PGM) in chromitites is also uneven, where large PGM aggregates have been reported in some chromitites, while no significant mineralization has been found in other chromitites. Another problem is the effect of hydrothermal processes overprinting the primary PGM (O'Driscoll and González-Jiménez, 2016; Palamarchuk et al., 2017; Sidorov et al., 2012; Tolstykh et al., 2015; Zaccarini et al., 2016) and influencing PGE budget (Li et al., 2013) in ultramafic rocks.

The Matysken complex (also called "Snegovoy") was described in the late 1980-s and is classified as an Ural-Alaskan type massif based on its structure, tectonic position, rock assemblage and geochemistry (Batanova and Astrakhantsev, 1992, 1994). Preliminary descriptions of PGM in the Matysken complex were provided by (Kutyev et al., 1991), and were subsequently described in a review devoted to interpreting the origin of silicate inclusions in PGM Kutyrev et al. (2020). In this paper, we present the results of an extensive study of the Matysken complex in terms of mineralogy and geochemistry in order to: (1) describe the PGE distribution in different units and constrain the role of chromitites and accessory chromian spinel in their accumulation, (2) define the order of PGM crystallization and their relationship with rock-forming minerals, (3) describe the formation and alteration of PGM during hydrothermal activity, and (4) constrain the source rock(s) for the Matysken River placer platinum.

2. Geological background

2.1. Koryak-Kamchatka platinum Belt

During the Mesozoic-Cenozoic, the Koryak-Kamchatka region formed an active margin in NE Asia that is now preserved in several magmatic, terrigenous and metamorphic terranes (Batanova and Astrakhantsev, 1992; Konstantinovskaia, 2001; Ledneva et al., 2000; Shapiro and Soloviev, 2009; Zinkevich and Tsukanov, 1992). One of these is the Achayvayam-Valaginsky terrane (AVT), which includes a number of sequences that were formed within intra-oceanic arc settings and accreted during the Paleocene-Miocene (Konstantinovskaia, 2001; Konstantinovskaya, 2011; Zinkevich and Tsukanov, 1992). Numerous zoned Ural-Alaskan type ultramafic complexes are spatially and temporally associated with the AVT, forming the Koryak-Kamchatka Platinum Belt, which stretches in a NE direction along the Kamchatka Peninsula (Fig. 1). Six groups of these complexes are known (Vildanova et al., 2002): South-Kamchatkan, North-Kamchatkan, Seinav-Galmoenan, Verkhne-Vyvensk, Epilchik and Tamanvayam (Fig. 1). The northernmost Epilchik group contains the Matysken complex, which is the subject of this study.

The host rocks for the Matysken complex include those of the Albian-Campanian Vatyna Formation, which consists of basalts with MORB geochemical affinity, interbedded with red jaspers, radiolarian cherts and hyaloclastites. The Vatyna Formation is considered to be an oceanic sequence preceding the formation of the arc (Batanova and Astrakhantsev, 1992). This is overlain by the Achayvayam Formation, which is comprised of basaltic and picritic volcanic rocks with island arc geochemical signatures (i.e. elevated large-ion lithophile elements and U content, negative Nb, Ta, Zr and Ti anomalies), interbedded with pyroclastic material and radiolarian cherts of Late Campanian to Paleocene age (Batanova and Astrakhantsev, 1992; Batanova et al., 2005; Kutyrev and Zhirnova, 2019; Vildanova et al., 2002).

2.2. Geology of the Matysken complex

The Matysken complex is comprised of an ultramafic body with almost ideal zoned structure (Fig. 1) and is exposed over an area of about 7 km^2. According to gravimetry, its depth is limited to ~ 1.5 km, where it is intersected by the Vatynsky regional thrust (Batanova and Astrakhantsev, 1992). The central part of the complex comprises a dunite core of ~2.5 km^2 area grading outwards successively to wehrlite, clinopyroxenite and gabbro (Batanova and Astrakhantsev, 1994). Boundaries between dunite and wehrlite are gradual; however, they are often masked by latter tectonic movements, which are expressed as serpentine breccias. Boundaries between dunite and clinopyroxenite are tectonic, although the latter form thin (0.1–1.0 m) dikes in dunite. Contacts of all ultramafic units with the host rocks of Vatyna Formation are tectonic, with no evidence of "hot" magmatic intrusion, such as quenching, porphyry textures and hornfels . On the contrary, gabbroic rocks show clear evidence of magmatic intrusion in the country rocks.

3. Methods and samples

3.1. Whole-rock chemistry

During fieldwork, dunite and wehrlite samples between 1.0 and 1.5 kg were collected and subsequently processed at the Institute of Volcanology and Seismology (Petropavlovsk-Kamchatsky, Russia). The rocks were sliced, then samples for PGE and Au analyses were ground into powder at the Geoscience Laboratories of Ontario Geological Survey (Canada) with the use of agate mills (in order to avoid contamination) and subsequently analyzed by inductively coupled plasma mass spectrometry (ICP-MS) after Ni-sulfide fire assay. The following elements were analyzed: Ru, Ir, Rh, Pt, Pd, and Au. Major and trace elements were analyzed in the Far East Geological Institute (Vladivostok, Russia). The following techniques were used: atom-emission spectroscopy after fusion with $LiBO_2$ for TiO_2, Al_2O_3, Fe_2O_3, MnO, MgO, CaO, Na_2O, K_2O, P_2O_5 (spectrometer iCAP 7600 DUO), "wet" chemistry with subsequent gravimetry for SiO_2 and chemically-bonded H_2O, and ICP-MS for all other elements (spectroscope Agilent 7500).

3.2. In-situ analytical techniques

Ordinary samples weighed between 1.0 and 1.5 kg, and in the case of rocks containing visible chromite mineralization, samples were between 5 and 10 kg. After collection, samples were divided into two parts. The first part was sliced into multiple 1–2 mm thick sections with a diamond saw. This method assisted in finding large platinum aggregates (>1.0 mm), which were visible to the naked eye. After polishing, numerous PGM between 1 and 250 μm in size were also visible. The second part of the samples was disintegrated into particles between 0.5 and 1.0 mm in size and then panned in order to separate heavy mineral concentrates, which were then studied by stereomicroscope to facilitate picking of individual PGM grains. Alluvial grains were processed the same way.

Polished samples, as well as platinum grains, were investigated in the Institute of Volcanology and Seismology FEB RAS by electron microscope Tescan VEGA-3. Wave-dispersion X-ray electron-probe microanalysis (EPMA WDS) of olivine and chromian spinel grains was carried out on a JEOL JXA-8320 microprobe at the Analytical Centre for Multielemental and Isotope Research at the V.S. Sobolev Institute of Geology and Mineralogy (AC IGM SB RAS), Novosibirsk, Russia. All analyses were performed using a beam diameter of 1 μm and accelerating voltage 20 kV. Beam currents during olivine and chromian spinel analysis were 100 and 50nA, respectively. Five WDS spectrometers were employed simultaneously with acquisition times for each element varying between 1 and 1.5 min. A set of well-documented, natural mineral compositions (olivine, chromite, ilmenite, Fe_2O_3 and TiO_2) were used as standards during EPMA and were analyzed every 40–60 spots.

The compositions of PGM were studied by energy dispersive X-Ray

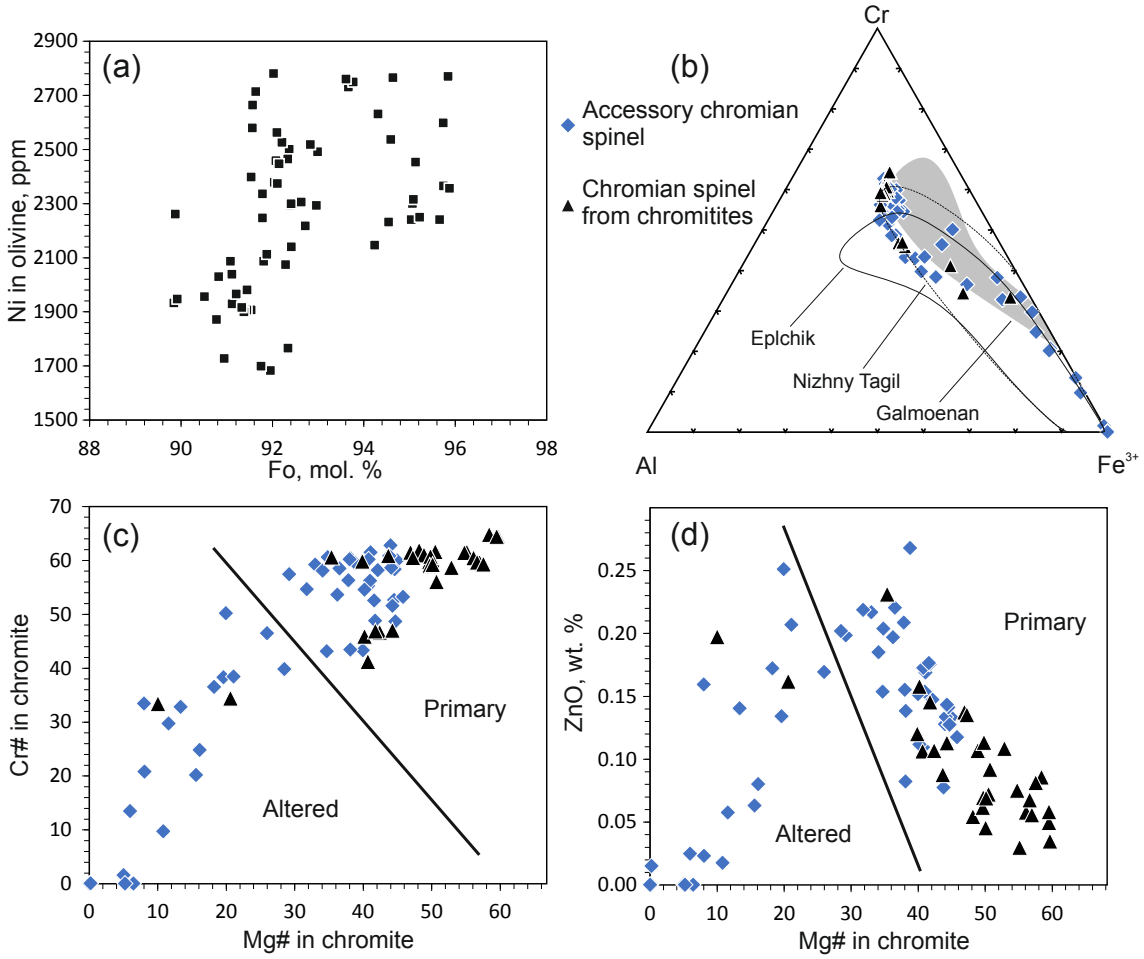

Fig. 2. (a) – Fo–Ni binary diagram for olivine from the dunite of the Matysken complex, (b) – ternary diagram for chromian spinel, (c, d) – binary diagrams for chromian spinel. Fields: Galmoenan (Sidorov et al., 2012), Epilchik (Kepezhinskas et al., 1993), Nizhny Tagil (Krause et al., 2007). The black line divides the fields of altered and primary chromian spinels.

Table 1
Composition of the Matysken complex ultramafic rocks.

#	Rock type	sample	SiO_2	TiO_2	Al_2O_3	Fe_2O_3	MnO	MgO	Ir	Ru	Rh	Pt	Pd	Au	Cr	Co	Ni
			weight %						ppb						ppm		
Detection limits			0.04	0.01	0.02	0.01	0.002	0.01	0.01	0.08	0.04	0.17	0.12	0.40	2.9	0.09	0.6
1	Dunite	M420	39.51	0.02	0.24	10.95	0.19	46.00	3.67	1.35	3.20	119.0	0.54	<0.40	7334	179.8	1509
2	Dunite	X210	38.12	0.02	0.30	10.06	0.18	44.85	2.34	0.92	1.96	78.3	0.33	0.40	4418	140.0	1283
3	Dunite	M352	39.38	0.01	0.20	11.23	0.19	46.16	2.13	1.01	2.71	107.0	0.50	<0.40	4988	146.2	1275
4	Dunite	M400	39.64	0.01	0.20	11.22	0.19	46.17	2.62	1.18	2.44	56.7	0.27	<0.40	4574	146.4	1198
5	Dunite	X182	40.28	0.05	0.34	9.67	0.17	44.65	2.38	1.10	1.67	71.7	0.55	2.00	3923	166.2	1515
6	Dunite	X196	39.37	0.01	0.23	10.75	0.20	46.23	4.45	1.52	2.96	119.0	1.14	0.60	5234	151.6	1352
7	Dunite	X187	39.05	0.03	0.45	10.42	0.18	45.58	3.13	1.00	1.78	55.8	0.71	0.60	4453	139.1	1392
8	Dunite	X275	39.00	0.01	0.16	10.67	0.19	47.67	1.93	0.98	2.05	40.9	0.28	0.40	3838	133.8	1181
9	Dunite	X250	39.57	0.02	0.30	10.25	0.19	45.87	1.74	0.75	1.36	7.3	0.06	0.60	3805	147.2	1539
10	Dunite	X236	39.34	0.01	0.09	10.32	0.19	46.16	1.91	0.72	1.41	22.0	0.16	0.40	3041	143.4	1367
11	Dunite	X349							1.82	0.66	1.64	35.3	0.44	1.20			
12	Wehrlite	X395	40.93	0.26	2.35	13.60	0.22	28.30	1.07	0.64	1.84	61.3	3.88	0.60	2845	142.1	628
13	Wehrlite	X362	49.52	0.17	1.35	6.45	0.12	21.61	0.21	0.32	0.77	35.5	1.45	<0.40	4031	73.6	402
14	Wehrlite	A159							0.38	0.50	1.83	67.6	1.36	0.60			
15	Wehrlite	X400	43.90	0.30	2.13	11.87	0.17	22.14	25.00	2.83	9.34	721.0	5.47	0.70	2021	116.2	523
16	Ref. material*								9.23	9.67	9.81	137	109	47.50			
17	Ref. material duplicate								8.80	10.90	9.50	129	106	48.00			

Note. Full data are represented in Supplementary Table S2. Empty cells = not analyzed. * Standard INTL-19-35344 was used by Ontario Geoscience Laboratories for Au and PGE.

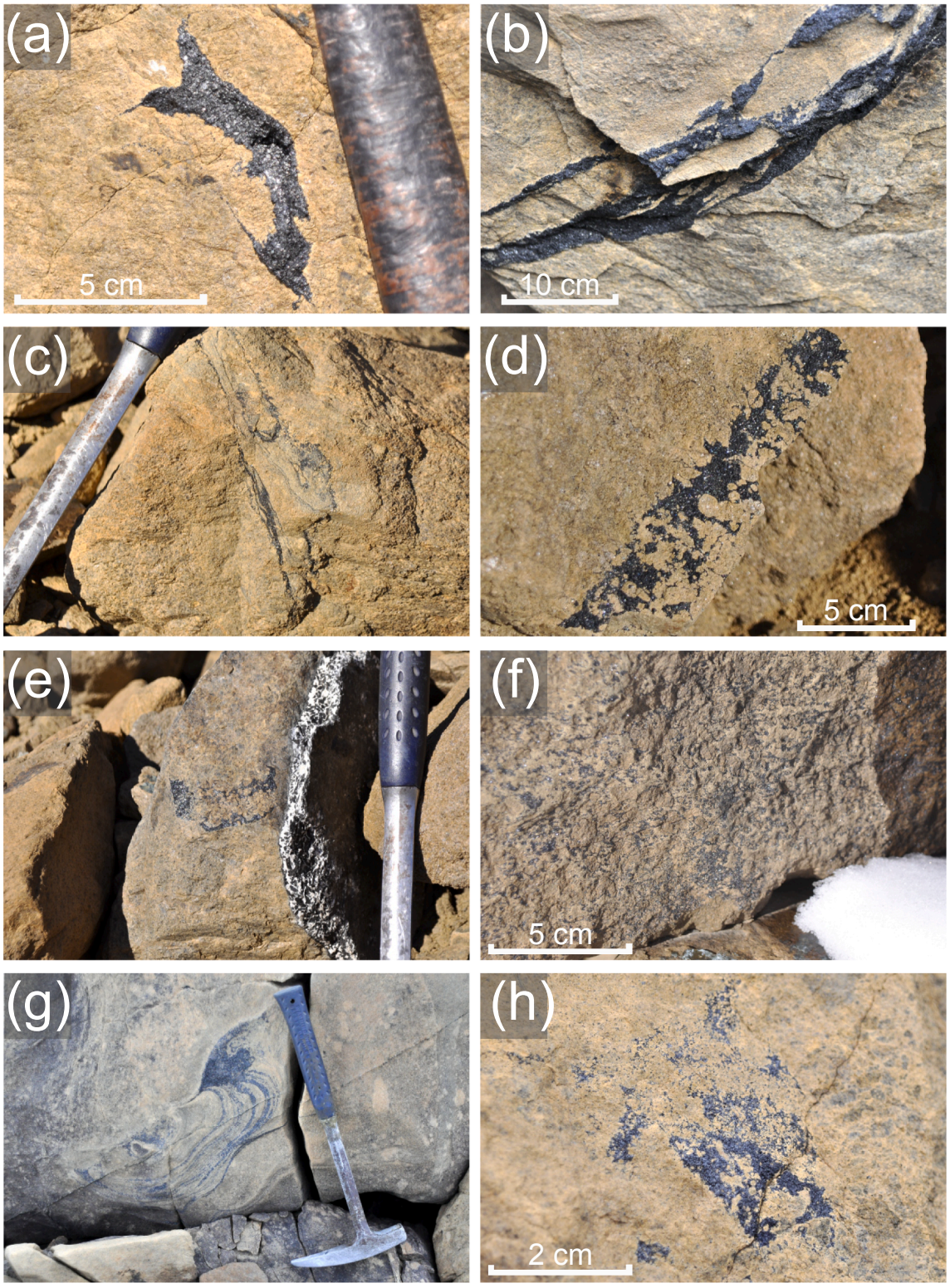

Fig. 3. Field photos of the Matysken complex chromitites: (a) – small chromitite schlieren, (b) – massive chromitite vein, (c) – set of thin chromitite veinlets, (d) – chromitite with euhedral olivine grains, (e) – banded chromitite at the contact with gabbroic dyke, (f) – disseminated mineralization, (g) – banded chromitite, (h) – transition of massive chromitite schlieren to the disseminated mineralization.

spectrometry using a Tescan VEGA-3 system equipped with Oxford XMax80 EDS detector. A beam accelerating voltage of 20 kV, a 20 s counting live time and 0.7nA current intensity were used. The following analytical lines of X-ray spectra were used to detect elements: Mα lines — for Pt, Os, and Ir; Lα lines—for Ru, Rh, Pd, and As; and Kα lines — for Fe, Cu, S, Ni, Al, Mg, Ca, V, Mn, Ti, Cr, and O. The following standards were used: pure metallic Pt, Os, Ir, Ru, Rh and Pd for PGE, sanidine for Si, K and Na, blue diopside for Ca, MgO for Mg, Al_2O_3 for Al, TiO_2 for Ti, $AlPO_4$ for P, V_2O_5 for V, rhodonite for Mn, FeS_2 for Fe and S, pure metallic for Ni.

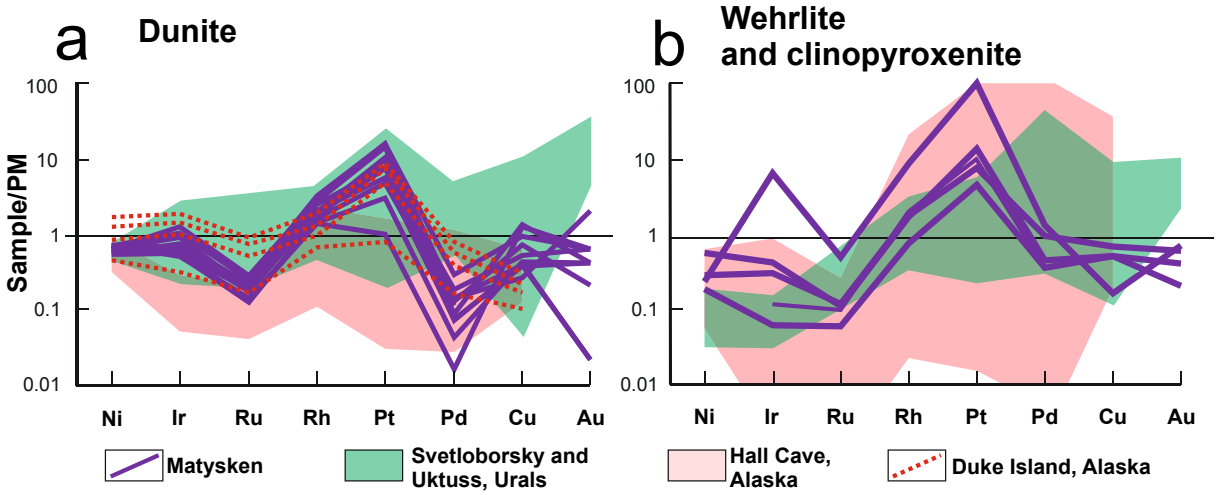

Fig. 4. Primitive mantle-normalized patterns of PGE and Au distribution in dunites and wehrlites of the Matysken and other Ural-Alaskan type complexes. Uktus and Svetloborsky after Garuti et al., 1997a, Hall Cave and Duke island after Li et al. (2013). Primitive mantle values after (Lyubetskaya and Korenaga, 2007).

4. Results

4.1. Petrography and mineralogy

Dunites in the field appear as homogenous, almost unaltered rocks. Despite serpentinization being significant near the marginal zones of the dunite core and along the deformation boundaries, the majority of dunite is exceptionally fresh with only thin serpentine veins observed. Common dunite in the Matysken complex is almost monomineralic and composed of olivine grains ranging from 2 to 3 mm in size. Coarser grained dunites (4–9 mm grain sizes) are less common, while pegmatoidal (>10 mm) and fine-grained (<2 mm) types are exceptionally rare. The only other mineral which may reach a few volume percent in dunite is chromian spinel. Rare individual grains of subhedral diopside or less common pargasite are also present in the dunite. Their abundance tends to be higher at the marginal part of dunite core, near the wehrlite units. Furthermore, these minerals often occur near chromitites. Sulfides are scarce (pentlandite dominates over pyrrhotite) and typically occur interstitial to olivine and clinopyroxene crystals. Olivine in dunites is high-magnesian (Fo mol.% = Mg/(Mg + Fe) = 0.90–0.96), with Ni content ranging from 1700 to 2800 ppm (Supplementary Table S1). Nickel and Fo show weak correlation at the range of Fo < 93 and no correlation at the range of Fo > 93 (Fig. 2a). The latter group represents olivines intergrowing with chromian spinel; therefore, their high Mg content may be explained by the re-equilibration of olivine (Ballhaus et al., 1991). In this case, Fe may diffuse into the latter, making olivine more magnesian without influencing Ni content. The whole-rock compositions of dunite are listed in Table 1.

Wehrlite is comprised of 10 to 40 vol% olivine, 60 to 80 vol% clinopyroxene and variable amounts of chromian magnetite and phlogopite. Clinopyroxene is subhedral to olivine and exists within interstitial spaces in the rock. Rare biotite- and amphibole-bearing wehrlites form irregular zones within the aforementioned more common wehrlite rocks.

Chromitites are restricted to the dunite core and show uneven distribution. A few regularities were observed during the field investigation, such as chromitites are much more abundant in the central parts of the complex and their abundance decreases towards the outer parts. At the same time, chromitites usually occur as clusters, where tens of them may occupy a relatively small area, while they are rare or absent in other areas of the complex. Morphologically, chromitites can be subdivided into several general types: schlieren (Fig. 3a, h), massive (Fig. 3b), banded (Fig. 3c, e, g), net-like, massive veins with olivine crystals (Fig. 3d) and disseminated (Fig. 3f, h). However, the margins between these types are indistinct and may transition from one to another (Fig. 3h). The thickness of chromitite accumulations does not exceed 10 cm, while their length is restricted to 1–2 m. Contacts between host dunite and chromitite may be sharp, as well as gradational from chromitite to dunite in chromian spinel-enriched dunite.

The compositions of accessory and chromian spinels from chromitite plot into two overlapping fields (Fig. 2b-d). For both unaltered accessory chromian spinels and those from chromitite, the Cr# (Cr/(Cr + Al), mol. %) ranges from 45 to 63, while spinel from chromitites have higher Mg# (Mg / (Mg + Fe), mol. %): 35–64 (29–45 for accessory chromian spinel). Minor component contents (e.g. Zn) are correlated with Mg# and do not provide any additional information that can be used to discriminate between accessory chromian spinel and chromian spinel from chromitite.

4.2. PGE distribution in dunite and wehrlite

Dunites and wehrlites share similar primitive mantle (PM)-normalized PGE patterns (Fig. 4). Platinum shows higher enrichment compared to other PGE in both rocks with average concentrations of 68 and 62 ppb for dunites and wehrlites, respectively. An exception is wehrlite sample "X400" with anomalously high content of 721 ppb Pt and was excluded from calculations involving PGE. Palladium is the most depleted of the PGE compared to the normalized mantle (Fig. 4) but is slightly higher in the wehrlites (average Pt/Pd ratio is 113 for dunite and 35 for wehrlite; Table 1). The PGE distributions in rocks of the Matysken complex are similar to those of the other Ural-Alaskan type complexes, including Uktus and Svetlobosky in the Ural Mountains (Garuti et al., 1997a), and Hall Cave and Duke Island in Southern Alaska (Li et al., 2013) (Fig. 4). The only principal difference is the Pd depletion, which is more significant for the Matysken complex.

Platinum and palladium are the most variable among PGE, where Pt contents in dunite ranges from 7.3 to 119.0 ppb and Pd from 0.06 to 1.14 ppb. Rhodium is of similar concentration (~1.8 ppb) for both rock types and is one order of magnitude less compared to the PM values. The Au content is of the similar PM-like values for both dunite and wehrlite (Fig. 4) and is independent of PGE concentration. Iridium and Ru are enriched in dunite (2.6 and 1.1 ppb on average, respectively) with respect to wehrlite (1.0 and 0.5 ppb on average, respectively). If compared with PM, Ir is of similar concentration and Ru in dunite is about one order of magnitude more depleted (Fig. 4a). These latter element contents show the smaller variations, ranging from 1.9 to 3.8

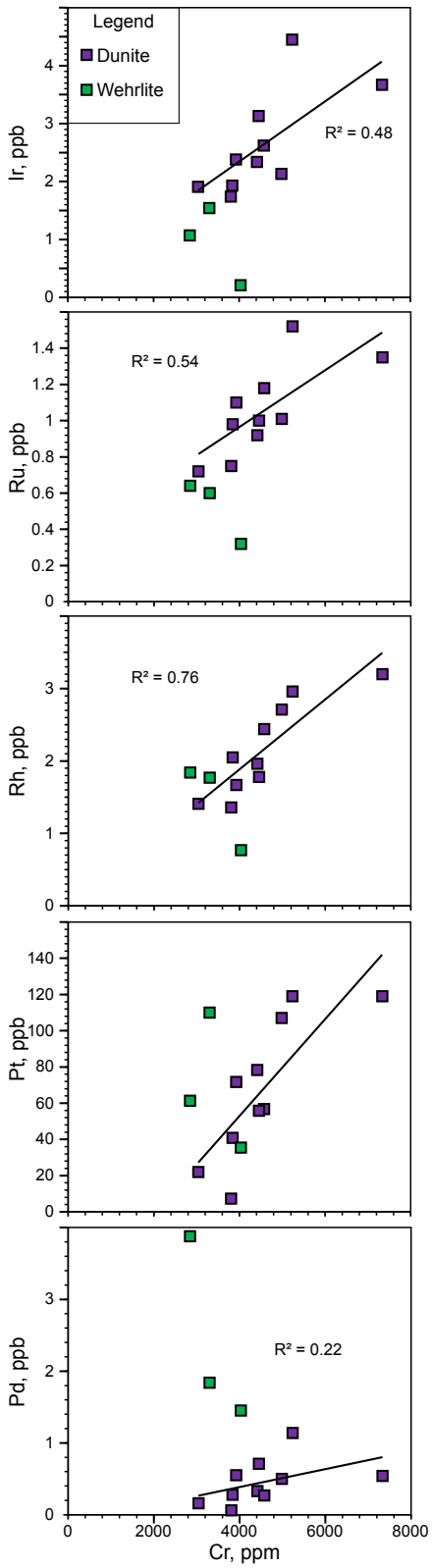

Fig. 5. Correlation between Cr and PGE in dunites (purple squares) and wehrlites (green squares). Trend lines and R^2 values are given for dunites only. (For interpretation of the references to colour in this figure legend, the reader is referred to the web version of this article.)

ppb for Ir and from 0.72 to 1.52 ppb for Ru. Similarly, Rh content does not show any strong variation, ranging from 1.4 to 3.2 ppb Rh in dunite (Fig. 4b, Table 1).

All PGE, with an exception of Pd, correlate positively with Cr in dunite; however, the correlation for all elements is not well pronounced and only reaches 0.76 (R^2) for Rh (Fig. 5). All other PGEs show a positive correlation with each other. The best correlations are observed for Ir-Ru and Pt-Rh pairs, while for other elements, strong deviations from the trend line are present.

4.3. Distribution of PGM and related minerals

Platinum-group minerals were observed in dunite and wehrlite. In dunite, they may occupy one of two principal positions: in chromitites, and in serpentine veinlets, while in wehrlite they are scarce and commonly associated with chromian magnetite segregations located in partly serpentinized olivine grains.

4.3.1. PGM in chromitites

Careful examination allows for finding small PGM grains in the order of first tens of μm (Fig. 6) in almost every chromitite sample, as well as rare larger aggregates in certain samples (Figs. 7, 8). The small grains form angular inclusions in chromite (Fig. 6a, b, d), while the larger ones occur at triple junctions between chromian spinel grains or as interstitial filling cementing individual spinel crystals (Fig. 7e-h). Direct contacts between isoferroplatinum and olivine are absent, because the space between these two minerals is occupied by thin serpentine fringes. Contacts between isoferroplatinum and pargasite were observed (Fig. 7h). The latter is euhedral and may be intergrown with cuproiridsite ($CuIr_2S_4$).

Native osmium, the second abundant PGM, is euhedral. It forms crystals that appear elongated or even acicular in polished sections (Fig. 8). However, the study of unpolished grains reveals that native osmium actually forms skeletal crystals consisting of planar lamellae which penetrate isoferroplatinum and the chromite matrix (Fig. 8d). Other common PGM include laurite RuS_2 and erlichmanite OsS_2. Laurite forms euhedral crystals with zoned structure that is clearly visible in BSE imaging, where dark areas are Os-poorer and light areas are Os-richer (Fig. 9b). In contrast, erlichmanite forms subhedral or anhedral grains, which may infill the intergranular space between chromian spinel crystals (Fig. 8e) or form elongated inclusions in isoferroplatinum (Fig. 8a).

Some isoferroplatinum crystals along their margins change to skeletal crystals (Fig. 9a) or euhedral grains (Fig. 9d). In these cases, isoferroplatinum is intergrown with hydrous silicates (serpentine or chlorite), pentlandite and pyrrhotite. In many cases, these aggregates transit to tetraferroplatinum towards the margin of the crystal (Fig. 9c).

Tetraferroplatinum, together with tulameenite and Cu-rich compounds, such as tomamaeite Cu_3Pt or an unnamed compound Cu_4Pt, are often found at the margins or fractures in isoferroplatinum, likely replacing it (Fig. 9e). Sperrylite and irarsite may often be found in fractures indicating a late origin (Fig. 9f).

4.3.2. PGM in serpentinite

In addition to chromitite, PGM can also be found in serpentinite (Fig. 9). Serpentinites of the Matysken complex can be subdivided into two groups. The first group represents very thin (mm) veinlets that transect olivine and chromian spinel. The serpentine often surrounds the chromitites, being located at the chromian spinel-olivine margin (Fig. 9c, g-i, k). The second group represents larger scale serpentinization, which is mostly restricted to the marginal parts of the dunite unit, or to zones of intense tectonic deformation. Field relations of the two serpentine types indicate that the first type formed prior to massive serpentinization. Platinum-group minerals mostly associate with the first group. Such PGM are commonly associated with sulfides, such as pentlandite (Fig. 9g-j), pyrrhotite and, occasionally, sphalerite (Fig. 9e).

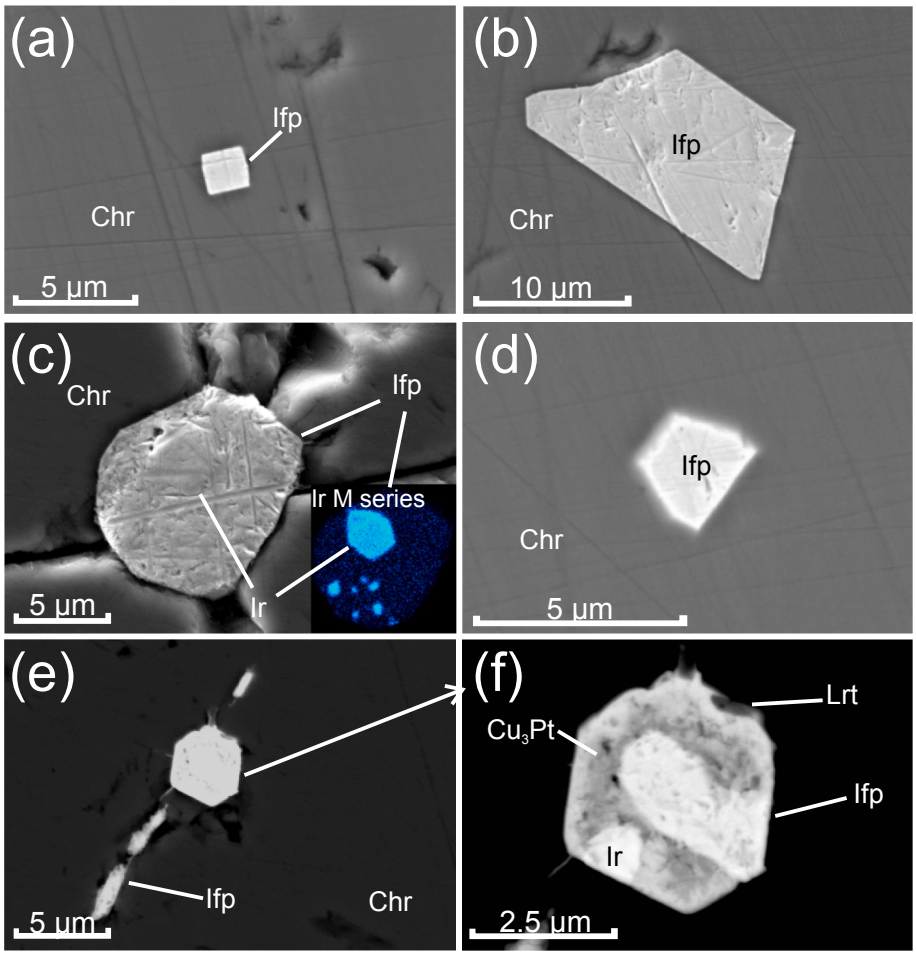

Fig. 6. (a, b) Euhedral isoferroplatinum (Ifp) inclusions in chromian spinel (Chr), (c) isoferroplatinum and native iridium (Ir) in a triple-junction of chromian spinel grains, inset represents Ir M series X-Ray intensity map, (d) minute isoferroplatinum inclusion in chromian spinel, (e) isoferroplatinum occurs along fractures in chromian spinel, (f) composite inclusion of isoferroplatinum, laurite (Lrt), native iridium and tomamaeite (Cu_3Pt). (a-d) Back-scatter electron (BSE) + secondary electron (SE) SEM images, (e, f) – BSE.

In this assemblage, isoferroplatinum is also a major mineral. Because of the textural differences, this form of isoferroplatinum is henceforth referred to as "isoferroplatinum-II". Similar to the above described large platinum aggregates, isoferroplatinum-II may be overprinted by secondary alloys of ferronickelplatinum (Fig. 9h) and tulameenite (Fig. 9i). A peculiar feature is shown in Fig. 9i where isoferroplatinum is replaced by tulameenite and the coexisting pentlandite crystal is altered to an unnamed compound Cu_4Pt near the contact with isoferroplatinum, and to awaruite in another part. Awaruite replacing pentlandite is very common in the Matysken complex, as well as for many other ultramafic rocks (Britten, 2017; Lawley et al., 2019; Sidorov et al., 2018; Zhu and Zhu, 2019). However, the awaruite-PGM association is not a common feature, as it has only been previously reported by Ahmed and Bevan (1981) and Sidorov et al. (2012). Other minerals associated with this type include hollingwhortite, irarsite (Fig. 9h), geversite (Fig. 9k) and Cu-Pt alloys with variable composition (Fig. 9k) and an unknown Pd-Bi phase (Fig. 9l).

4.3.3. PGM in wehrlite

Despite the elevated Pt content in one of the wehrlite samples (≈ 0.7 ppm), only small (<2 μm) PGM grains were found in the minute Cr-magnetite chains (Fig. 10). The only grain large enough to be analyzed by EDS (4 μm) corresponds to the formula $(Pt_{2.08}Sn_{0.40}Pd_{0.30}Rh_{0.05}Ru_{0.04}Ir_{0.03})_{2.94}(Fe_{0.94}Ni_{0.10}Cu_{0.02})_{1.06}$ (Supplementary Table S3), which resembles isoferroplatinum (Pt_3Fe) but with Pt substituted for Sn and Pd.

4.4. Placer platinum

Platinum-group minerals grains from the Matysken River are commonly up to 1 mm in size. They are moderately-rounded and represented by isoferroplatinum exclusively, whereas other minerals only occur as inclusions or intergrowths. In most cases, evidence of the primary shape is still present, such as planar facets that could correspond to cubic or octahedron shapes (Fig. 11a, c), polycrystalline structure (Fig. 11d), inclusions of native osmium (Fig. 11a, c) and chromian spinel (Fig. 11b). Other grains are more rounded and probably experienced higher degrees of abrasion due to longer transportation times (Fig. 11e). Among isoferroplatinum, a single grain of well-rounded awaruite coated with an unidentified compound, possibly stannopalladinite $(Pd,Cu)_3Sn_2$, was found (Fig. 11f).

5. Composition of PGM

5.1. Native metals and alloys

Pt-Fe minerals. The most abundant Pt-Fe mineral in chromitites has composition close to Pt_3Fe, with some deviations towards the Fe-enriched field (Fig. 12a, Supplementary Table S4). According to the previous studies (Cabri and Feather 1975, Malitch and Thalhammer 2002), the cubic Pt-Fe alloys occur as the following species: 1) cubic disordered native platinum with Pt content > 80 at.%; and 2) cubic ordered isoferroplatinum with Pt-content close to stoichiometric 75 at.%. The identification of mineral species ideally should be based on both composition and structural studies; however, in the absence of the latter,

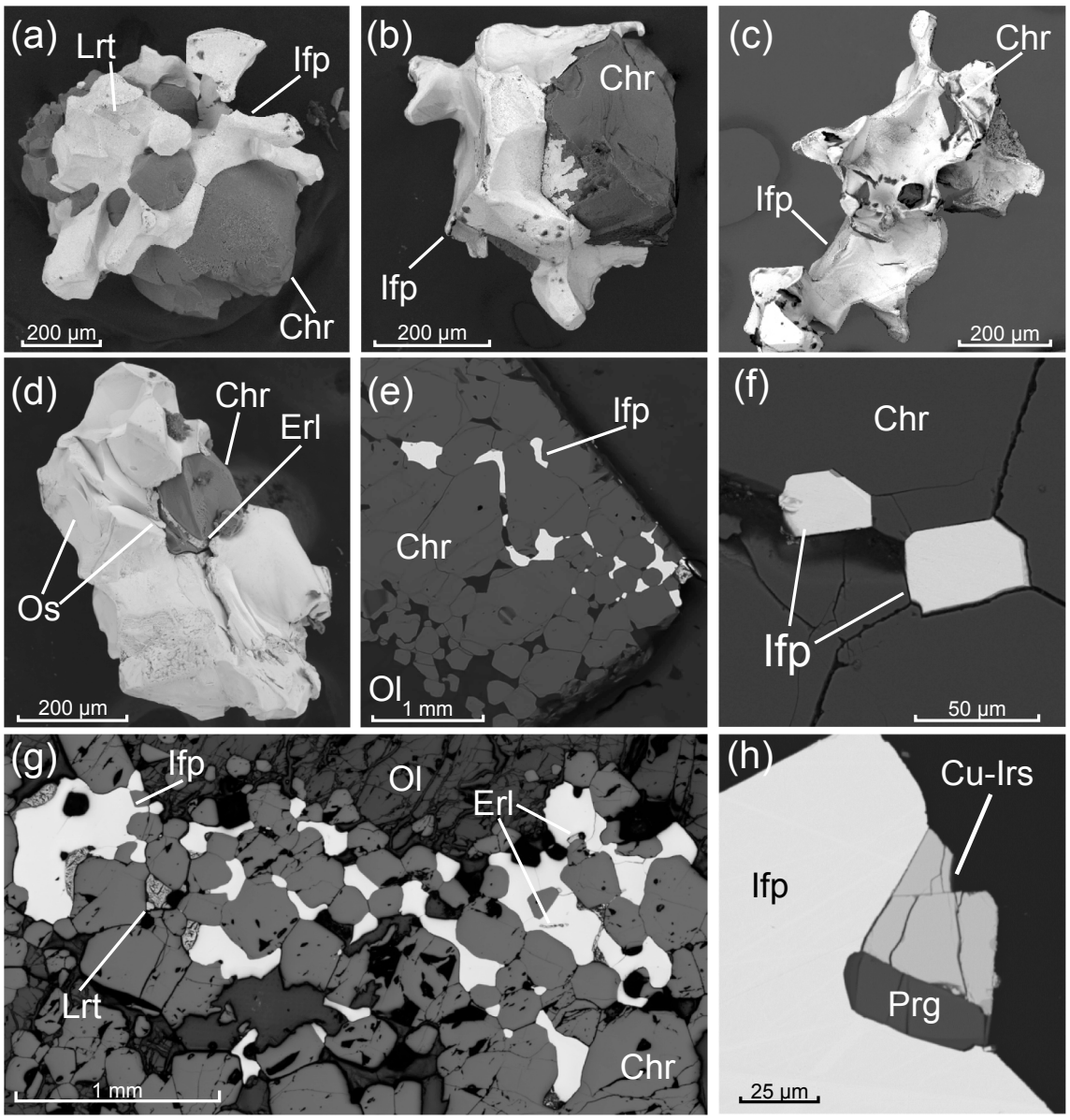

Fig. 7. Isoferroplatinum – chromian spinel aggregates from the Matysken complex: (a) intergrowth of isoferroplatinum (Ifp), chromian spinel (Chr) and erlichmanite (Erl), (b-d) – isoferroplatinum – chromian spinel intergrowth, (e-g) – polished sections of extremely Pt-rich chromitites (Ol – olivine), (h) isoferroplatinum at the junction of chromian spinel grains. All figures but "g" are back-scatter electron (BSE) SEM images, where "g" is in reflected-light. Figures "a", "b", "d", "e" represent unpolished grains, others – polished ones.

compositions observed more likely correspond to isoferroplatinum. The composition of isoferroplatinum from lodes is close to those from placer, where the only principal difference is wider spread of the latter (Fig. 12). The Cu content in isoferroplatinum reaches up to 2 wt%, while most compositions fall in the range of 0.2–1.0 wt% Cu. Among PGE, the main impurity in isoferroplatinum is Ir, which can reach up to 5.8 wt%, while most of the analyses show Ir content from 0.2 to 4.0 wt% (Fig. 12b). Both Pd and Rh contents barely reach 1.0 wt% (Fig. 12c, Supplementary Table S4) and in the majority of analyses are not detected. Osmium was not detected in most grains and rare analyses with 0.2–1.0 wt% Os were treated tentatively because of the presence of very abundant, ultra-thin native osmium lamellae (Fig. 8d, f), which may have affected the acquisition of the X-ray spectrum.

Other alloys are represented by tetraferroplatinum, tulameenite and tomamaeite and an unnamed Cu_4Pt compound (Fig. 12a). Tulameenite and tetraferroplatinum form a solid solution series with a continuous range of intermediate compositions (Fig. 12a). Unlike isoferroplatinum, these alloys do not bear significant amounts of other PGE (Fig. 12b, c, Supplementary Table S4).

Os-Ir-Ru alloys are widely distributed within the studied assemblage, but their abundances are significantly lower than those of Pt-Fe alloys. According to the classification of Harris and Cabri (1991), Os-Ir-Ru alloys are represented by native osmium and native iridium divided by an immiscibility gap (Fig. 13a). Minerals occur in both lode and placer assemblages, however, native iridium from lodes is too small to be quantitively analyzed and was thus not indicated in the diagram. Both minerals contain low concentrations of Ru (Fig. 13a, Supplementary Table S5), which is in accordance with the low whole-rock Ru content (Fig. 4a, Table 1) and is typical for Ural-Alaskan type complexes (Tolstykh et al., 2002a). Iridium content in coexisting Os-Ir-Ru and Pt-Fe alloys shows an excellent correlation (Fig. 13) suggesting that they formed under equilibrium conditions.

Os-Ir-Rh-Fe alloys are represented by hexaferrum (Fe,Os) (Supplementary Table S5, no 34–36). It has typical composition (Cabri and

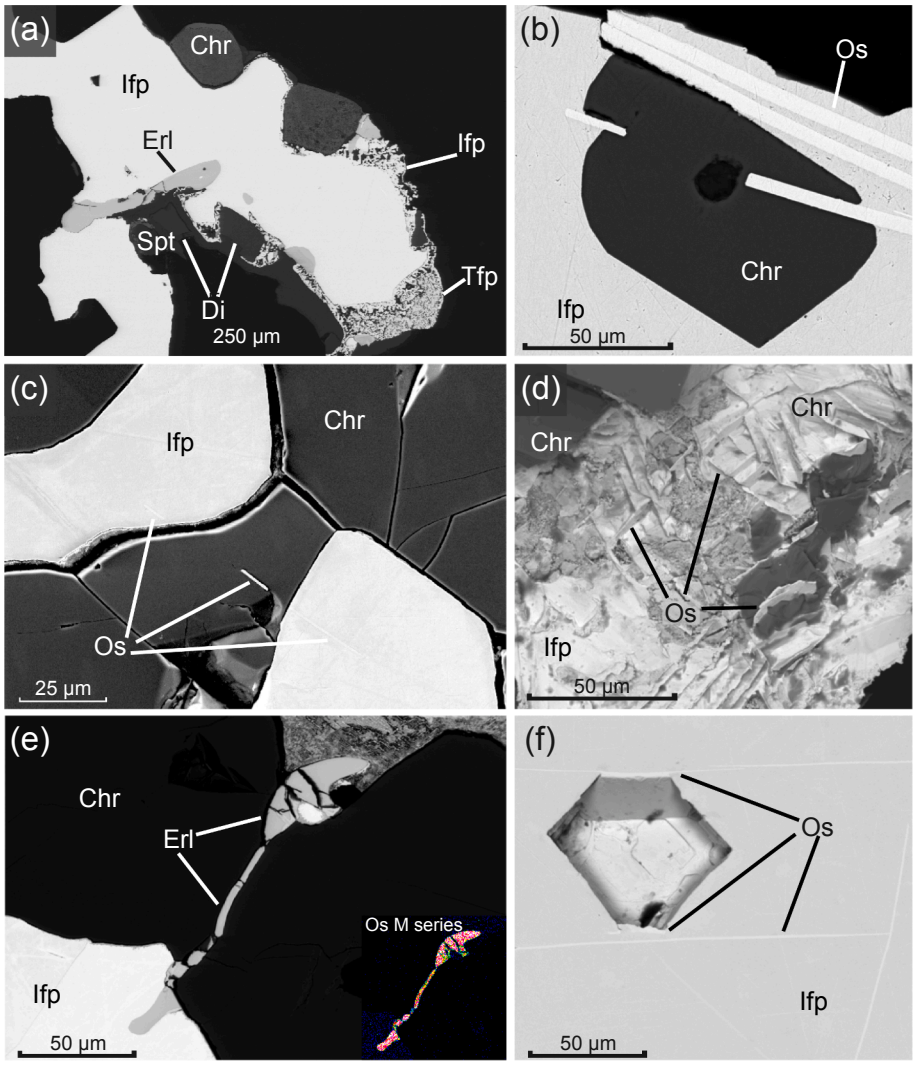

Fig. 8. Back-scatter electron (BSE) images of isoferroplatinum (Ifp) intergrowths with native osmium (Os) and erlichmanite (Erl): (a) – Isoferroplatinum intergrown with chromian spinel (Chr) and diopside (Di) with inclusions of erlichmanite and rims of skeletal isoferroplatinum and tetraferroplatinum (Tpf), (b,c) – native-osmium crystals euhedral to both isoferroplatinum and chromian spinel, (d) – parallel-aligned superfine native osmium lamellae transecting chromian spinel, (e) – erlichmanite in the interstitial space of two chromian spinel grains, inset represents Os Mα X-Ray intensity map, (f) – superfine native osmium lamellae controlling the shape of the cavity in isoferroplatinum. The lamellae had already formed prior isoferroplatinum crystallization. All images but "d" are polished sections, where "d" is an unprepared grain.

Aiglsperger, 2018) with 33 wt% Fe, 60 wt% Os and minor impurities of Rh (up to 2 wt%) and Ir (1.8–3.8 wt%). The only unusual constituent is 1.3–1.6 wt% S, which may be explained, as hexaferrum is often described to be the result of laurite-erlichmanite series mineral alteration (Mochalov et al., 1998), and thus the impurity may represent a fingerprint of this process.

5.2. Sulfides, arsenides, sulfarsenides and other minerals

Sulfides are represented by two abundant minerals, laurite RuS_2 and erlichmanite OsS_2, along with lesser amounts of boweite Rh_2S_3), thiospinel group member cuproiridisite $CuIr_2S_4$ and very scarce cooperite PtS. Laurite and erlichmanite form the solid solution series with a compositional gap between ~0.25 and 0.40 f.u. Os (Fig. 13b, Supplementary Table S6). This gap divides the two morphological types described above. Euhedral zoned crystals of laurite/erlichmanite (Fig. 11b) correspond to the Ru-rich area of the ternary diagram (Fig. 13b), while subhedral or anhedral grains, which may infill the intergranular space between chromian spinel grains or even form veinlets, are always close to the erlichmanite endmember (Fig. 13b). Bowieite corresponds to the empirical formula $(Rh_{1.00}Ir_{0.98}Ru_{0.02}Pd_{0.02})_{2.02}S_{2.98}$, which is in the middle member of bowieite Rh_2S_3 – kashinite Ir_2S_3 solid solution series (Supplementary Table S7). Cuproiridsite, among Cu, Ir and S, has up to 18.5 wt% Pt, 12.9 wt% Rh and 1.9 wt% Fe and thus corresponds to the intermediate member of the cuproiridsite $CuIr_2S_4$ – malanite $CuPt_2S_4$ – cuprorhodsite $CuRh_2S_4$ solid solution (empirical formula $(Cu_{0.79}Fe_{0.19})_{0.98}(Ir_{0.89}Rh_{0.64}Pt_{0.51})_{2.04}S_{3.98}$). Cooperite, unlike these minerals, is scarce and was determined only qualitatively due to the small grain size.

Arsenides and sulfarsenides are represented by irarsite and subordinate sperrylite. Cases where their sizes are large enough for the quantitative compositional measurement are scarce. Irarsite corresponds compositionally to the intermediate member of the irarsite IrAsS – platarsite PtAsS solid solution series $(Ir_{0.52}Pt_{0.39}Rh_{0.08})_{0.99}As_{0.96}S_{0.97}Sb_{0.04}Te_{0.04}$. The composition of sperrylite was not measured due to its small size (Fig. 11f).

Other minerals: Tellurides are scarce in the Matysken complex. Only one grain of an unknown compound was found and was shown to correspond to the following formula: $(Ir_{048}Bi_{0.30}Pt_{0.17}Rh_{0.06})_{1.01}(Te_{0.66}Sb_{0.16}S_{0.11}As_{0.06})_{0.99}$. *Antimonides* were only encountered once. Geversite $PtSb_2$ forms submicron scale inclusions in pentlandite or is intergrown with sphalerite and an undefined Cu-Pt alloy (Fig. 9j, k), but was not analyzed due to its small size.

6. Discussion

6.1. Comparison between placer and lode PGM assemblages

Two contrasting models have been proposed for the formation of placer PGM (Bowles et al., 2017). The first one involves primary

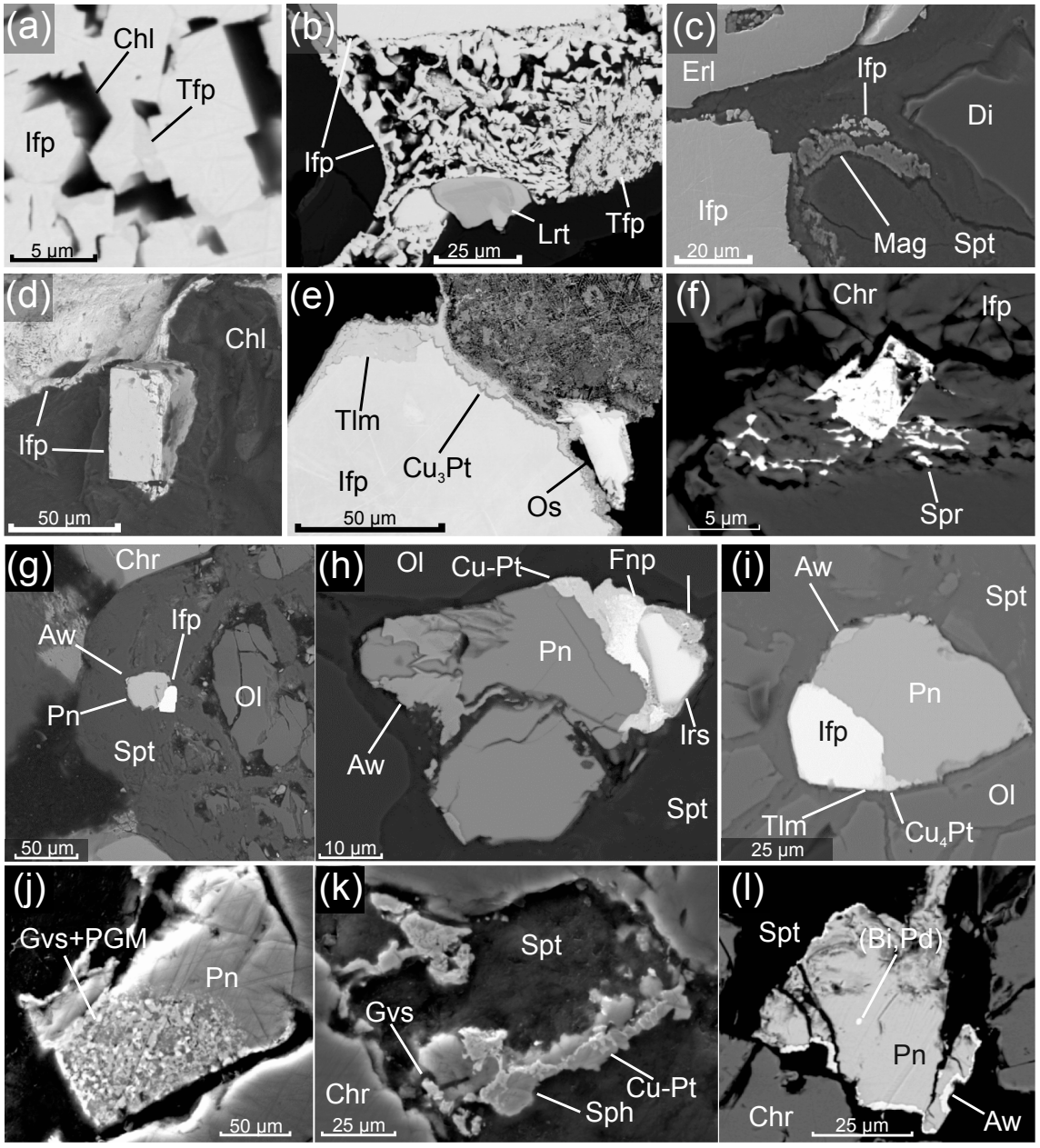

Fig. 9. Back-scatter electron (BSE) SEM images showing the PGM relationship to serpentine veinlets: (a,b) – skeletal isoferroplatinum-II overgrowths isoferroplatinum-I (Ifp) and pyrrhotite (Po) inclusion, note the zonal laurite (Lrt) crystal with Os-enriched outer rim; (c) – euhedral isoferroplatinum crystal in the serpentine (Spt) matrix near magnetite (Mag); (d) euhedral isoferroplatinum crystal in chlorite (Chl) matrix, (e) isoferroplatinum with rim of tulameenite (Tlm) and tomamaeite (Cu_3Pt); PGM in serpentine veinlets: (f) – isoferroplatinum inclusion and sperrylite (Spr) veinlets in fractured chromian spinel (Chr), (g) – intergrowth of isoferroplatinum (Ifp), pentlandite (Pn) and awaruite (Aw), (h, i) – same as "g" with greater mineral diversity (Fnp – ferronickelplatinum, Hwt – hollingwhortite, Irs – irarsite), (j) – pentlandite substituted by a microaggregate of geversite (Gvs) and various undistinguishable PGM, (k) – geversite, sphalerite (Sph) and undefined Cu-Pt alloys in serpentine veinlet, (l) pentlandite with awaruite and inclusion of unnamed Bi-Pd phase.

formation of PGM within the ultramafic complex, followed by their redistribution by weathering and subsequent mechanical transport without any alteration besides surface abrasion (e.g. Cabri et al., 1996; Tolstykh et al., 2004). The second model involves PGE solution during weathering, possibly aided by high Eh and low pH conditions together with biochemical leaching (Bowles et al., 1986, 2017). However, the second model demands hot and wet climate, favoring the formation of laterites (e.g. Bowles et al., 2017), which is unlikely for Koryak highlands. The Northern Segment of the Achayvayam-Valaginsky terrane was emplaced during the Mid Eocene and for the majority of its history existed in the latitudes of about 60°N (Konstantinovskaia, 2001) in moderate or subarctic climate. Comparisons between lode and placer PGM also support the first model.

In both lodes and placers, the dominant mineral is isoferroplatinum, which is mantled by tetraferroplatinum, tulameenite and ferronickelplatinum, and contains inclusions of native osmium and native iridium (Table 2). Skeletal rims of isoferroplatinum-II occur in both lodes and placers (compare Figs. 9a-c and 11f). The compositions of lode and placer mineral assemblages are also very similar, where the only difference is that the latter comprise the set of the isoferroplatinum grains with high Pd (>1 wt%) and Ir (>4 wt%) (Figs. 12, 13). Platinum-iron alloys in placers related to the deeply eroded complexes typically have higher contents of Fe and Ir, and lower contents of Pd compared to the complexes that exhibit low levels of erosion (Nekrasov et al., 1994;

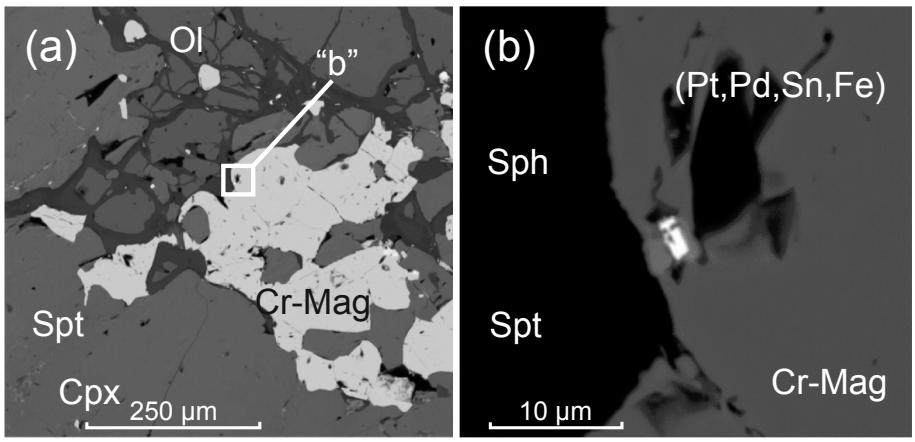

Fig. 10. Back-scatter electron (BSE) SEM images of PGM in wehrlite: (a) – general view of Cr-magnetite (Cr-Mag) schlieren and serpentine (Spt) veinlets at the boundary between clinopyroxene (Cpx) and olivine (Ol) crystals with image "b" location marked by a rectangle, (b) – intergrowth of Pt-Pd-Sn-Fe alloy, sphalerite (Sph) and Cr-magnetite.

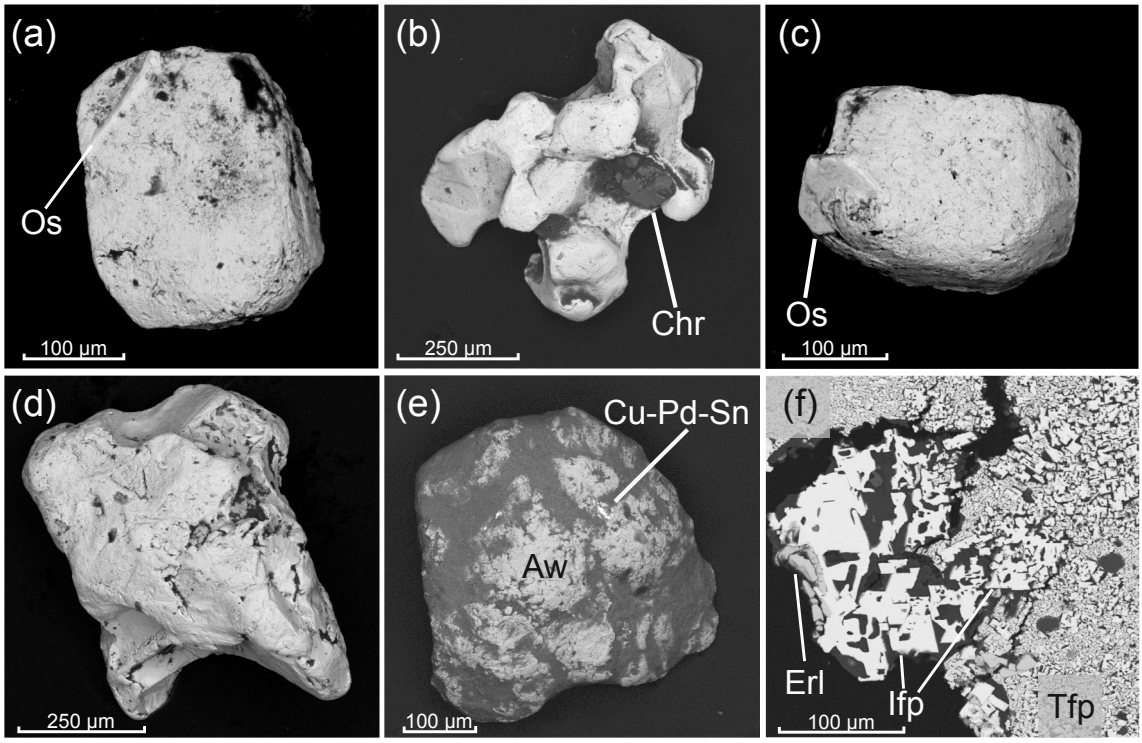

Fig. 11. Back-scatter electron (BSE) SEM images of isoferroplatinum (a-d) and awaruite (e) grains from the Matysken River, and isoferroplatinum and tetraferroplatinum skeletal crystals in polished sections(f). Dark areas in a-e are fluvial coating of silicate minerals, on f – chlorite, serpentine and pentlandite. Mineral abbreviations: Os -native osmium, Chr – chromian spinel, Aw – awaruite, Cu-Pd-Sn – unnamed alloy, Erl – erlichmanite, Ifp – isoferroplatinum, Tfp – tetraferroplatinum.

Sidorov et al., 2012, 2019; Tolstykh et al., 2004). Therefore, we suggest that the exclusive presence of abnormally Pd- and Ir-enriched isoferroplatinum in the placers is the result of a longer history of erosion, where alluvium accumulation led to mixing of material derived from the various levels of, thereby resulting in the broader compositional variations in minerals of the placer assemblage compared to those of the lodes.

The occurrence of PGM in wehrlite and clinopyroxenite in Ural-Alaskan type complexes are rare, but for several placers these rocks were considered to be the single source, or in combination with dunite (e.g. Tolstykh et al., 2000). The only PGM reported in the Matysken complex wehrlite so far is an unnamed Pt-Fe-Sn-Pd alloy (Fig. 10, Supplementary Table S3), which was not observed in placers. Relatively high Pd/Pt ratios (Fig. 4) also suggest that in every wehrlite sample, PGM should be enriched in Pd compared to dunites samples. This is in accordance with the aforementioned regularity, where Pt-Fe alloys from placers related to the less-eroded, complexes (which bear significant amounts of wehrlite and clinopyroxenite), commonly have elevated Pd contents (Nekrasov et al., 1994; Sidorov et al., 2012, 2019; Tolstykh et al., 2004). Wehrlite and clinopyroxenite units were suggested to be the main source for Pd-rich PGM of Pustaya River (Tolstykh et al., 2000), Itchayvayam River (Sidorov et al., 2019) and Prizhimny Creek (Kutyrev

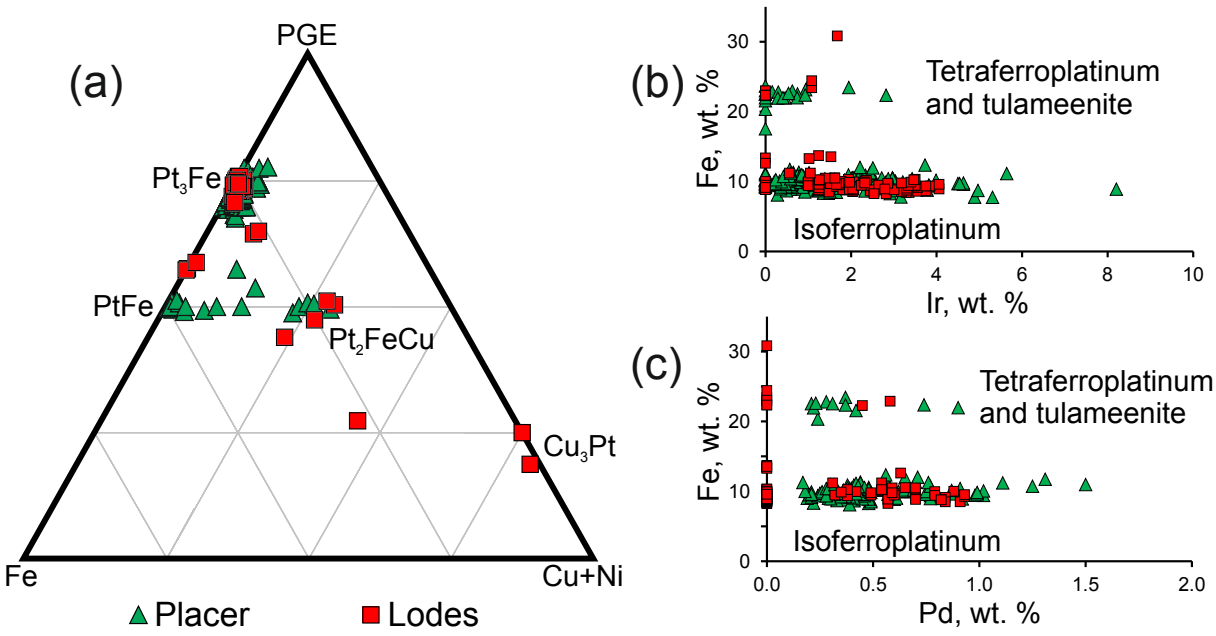

Fig. 12. Pt-Fe alloys composition.

et al., 2018) in the Koryak Highlands, and similar regularities have been reported for the lode ores of the Galmoenan complex (Mochalov, 2013). However, the vast majority of the Pt-Fe alloys found in placers have Pd-content of the same range as for Pt-Fe alloys from lode dunitic samples. Therefore, the only significant source for the placer association is dunite of the Matysken complex.

6.2. Chromian spinel control of PGE mineralization in dunite

Previously published data on Ural-Alaskan type complexes have shown that PGE tend to accumulate in chromitites located in dunites (Augé et al., 2005; Razin, 1976; Thakurta, 2018; Tolstykh et al., 2015; Vysotsky, 1913). This is strongly supported by mineralogical observations in our samples. Among the samples studied, only those which contain massive chromitites or chromite schlierens contain large platinum grains, such as those shown in Fig. 8, thereby confirming chromian spinel as a control on PGM precipitation. Furthermore, relatively large massive chromitites may both contain areas of extremely rich mineralization, as well as areas completely devoid of PGM. Among >90 chromitite samples whose mineralogy was investigated, only 4 contained PGM grains >0.5 mm in size (Fig. 7 and 8), while the majority of them contain only minute PGM grains (Fig. 6). A study of the variations of Pt contents in dunite of the Galmoenan complex showed that only analyses of samples >250 kg provided reproducible results (Nazimova et al., 2011). This is because Pt in chromitites tend to form relatively large and unevenly distributed segregations. Analyses of "barren" dunite, where only accessory chromian spinel is present, showed positive PGE–Cr correlations for all elements except Pd, which means that disseminated accessory chromian spinel uniformly concentrates Ru, Ir, Rh and Pt (Fig. 5). This presents an opportunity to calculate the amount of Pt concentrated in accessory spinel and compare it with those of chromitite.

Even massive chromitites normally comprise large amounts of olivine. Moreover, the sampling process implies processing chromitite together with the surrounding dunite. Therefore, we have taken 50 wt% of chromian spinel as a value roughly corresponding to the average chromitite sample analyzed. Average Cr_2O_3 content in the Matysken unaltered chromian spinel is 39 wt% (Supplementary Table S1), which gives ≈20 wt% Cr_2O_3 for such chromitite. These values are close to those reported by Nazimova et al. (2011). Further calculations show that such chromitite will contain ~3.3 ppm Pt, which is close to the Pt content reported for analogous chromitites of the Galmoenan Complex (first ppm, Fig. 4 in Nazimova et al., 2011), Nizhniy Tagil and Veresovoborsky complexes (Augé et al., 2005). The use of the regressive equation calculated by (Nazimova et al., 2011) that was formulated on the basis of a more significant data array, provided similar values (~6.2 ppm). Therefore, the principal difference between mineralization of accessory chromite and chromitites is the distribution of PGE, but not their absolute contents. Acquired data are in agreement with the study of Pushkarev et al. (2007), who examined chromitites of the Nizhniy Tagil complex and calculated that if 50% Pt and Cr_2O_3 is extracted from 260 m^3 of dunite with 0.3 wt% Cr_2O_3 and 0.05 ppm Pt, then 1 m^3 of ore with 30% Cr_2O_3 and 5 ppm Pt could be formed. In other words, both Pt and Cr were concentrated by a factor of 100.

6.3. Genetic implications

There is still no clear consensus on the origin of isoferroplatinum and chromian spinel intergrowths in Ural-Alaskan type complexes. For instance, some researchers suggest that PGM crystallized from a silicate melt with subsequent mechanical accumulation (Augé et al., 2005), or from late residual melts enriched in PGE and Cr (Nixon et al., 1990; Okrugin, 2011; Stepanov et al., 2020; Tolstykh et al., 2015), while others argue for a non-magmatic origin for mineralization (Mochalov, 2013; Pushkarev et al., 2007, 2015). These topics were reviewed in (Kutyrev et al., 2020), and the discussion below will be focused on cases where there is significant evidence for a non-magmatic origin of PGM origin (i.e. hydrous silicate and PGM intergrowths).

The possibility of PGE migration in hydrothermal fluids has been discussed extensively in the literature. Numerous work based on textural observations gave evidence of newly-formed PGM in various serpentinized ultramafic rocks (e.g. Betekhtin, 1954; Cabri and Genkin, 1991; Nixon et al., 1990; González-Jiménez et al., 2010, 2015). On the other hand, many works, including the recent ones critique the possibility of major PGE redistribution via hydrothermal processes on the basis of low PGE solubility in aqueous fluids (e.g. Barnes and Liu, 2012; Scholten et al., 2018). Additional natural evidence of potential PGE mobility under hydrothermal conditions is provided by studies of copper

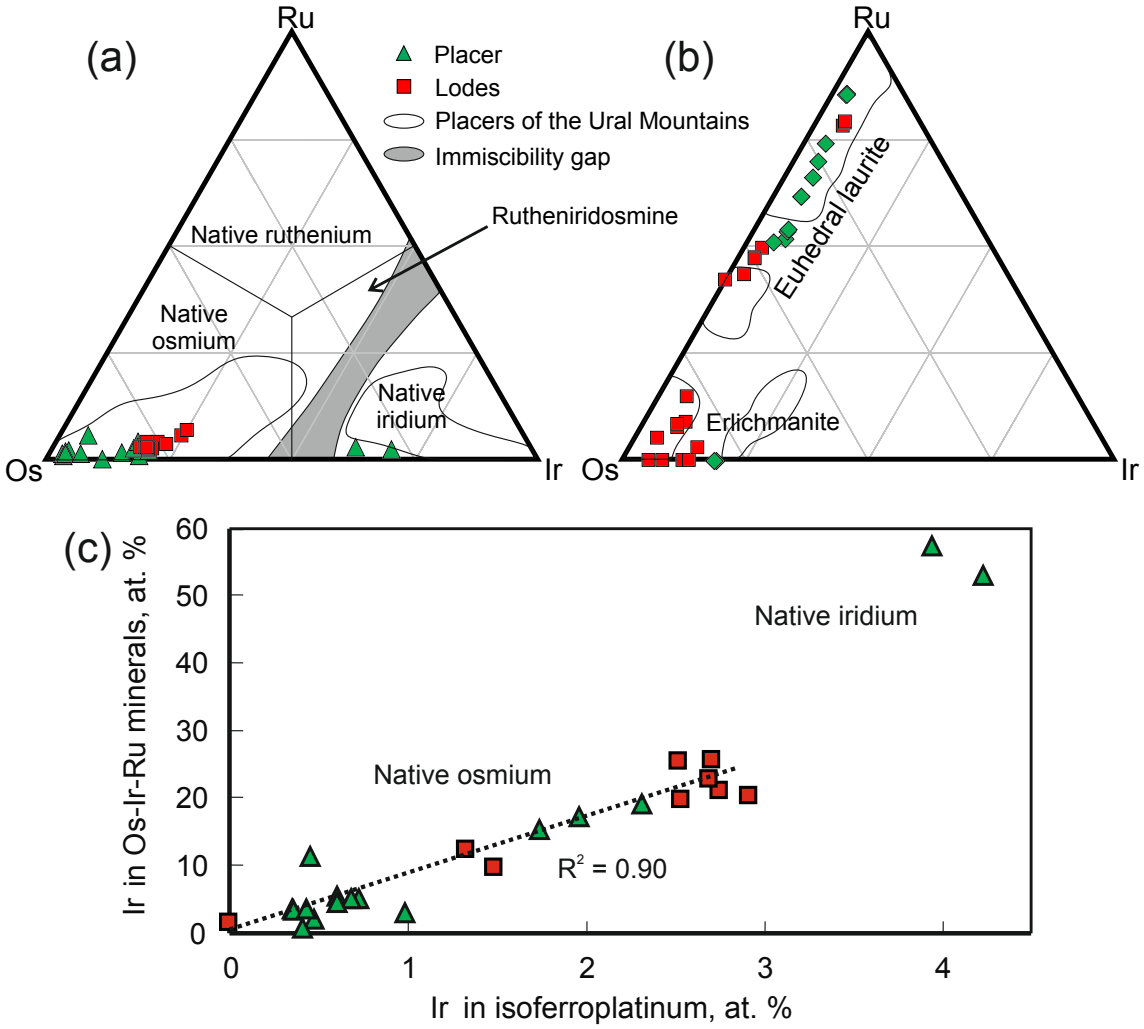

Fig. 13. Ternary diagrams of Os-Ir-Ru alloys (a) and laurite-erlichmanite (b) composition. In figure "b" minerals are subdivided into two groups: euhedral laurite, which is supposed to be an early forming mineral that crystallized together with the Os-Ir-Ru alloys, and erlichmanite, which forms rims or veinlets rather than euhedral crystals, (c) Ir content in coexisting isoferroplatinum and Os-Ir-Ru alloys (native osmium and native iridium), R^2 factor is given for native osmium-isoferroplatinum pairs only. Data for Ural Mountains after (Stepanov et al., 2020).

porphyry deposits, where Pd and, to a lesser extent, Pt may be concentrated in hydrothermal assemblages (Augé et al., 2005; Hanley, 2005; Tarkian and Stribrny, 1999), and hydrothermal Waterberg platinum deposit, South Africa (Oberthür et al., 2018). Below we discuss textural evidence for PGE hydrothermal redistribution in the Matysken complex.

In addition to isoferroplatinum forming intergrowths with chromian spinel, identical to those reported in other Ural-Alaskan type complexes (e.g. Augé et al., 2005; Nazimova et al., 2011; Tolstykh et al., 2015), the Matysken complex comprises isoferroplatinum-II, which is represented by intergrowths of pentlandite with euhedral isoferroplatinum nuggets in serpentinized olivine (Fig. 9g, i), skeletal isoferroplatinum intergrowths with pentlandite and chlorite at the marginal parts of larger grains (Fig. 9a-c), and perfect euhedral isoferroplatinum crystals in the serpentine matrix (Fig. 9c, d). All these cases share common features:

(1) All isoferroplatinum grains are euhedral or at least have euhedral facets that indicate formation in the presence of open space suitable for ideal crystal growth.
(2) Euhedral isoferroplatinum grains are intergrown with hydrous silicates (serpentine or chlorite), and often with pentlandite.

These common features indicate that this type of isoferroplatinum may have formed under different conditions than isoferroplatinum intergrown with chromian spinel. The rare but still evident occurrences of isoferroplatinum forming veinlets in chromian spinel (Fig. 8e) suggests that this isoferroplatinum-II may be considered to be related to serpentinization, which is probably associated with the redistribution of PGE. This is also supported by textural observations showing the presence of isoferroplatinum in fractures in chromian spinel (Fig. 6e).

Other minerals showing a strong affinity with serpentine are Fe- and Cu-rich alloys, including tetraferroplatinum, tulameenite, tomamaeite, unnamed Cu-rich compounds and less abundant minerals, such as irarsite, sperrylite and geversite. Tulameenite and Pt-bearing native copper have been previously reported in Tulameen district (British Colomia), where they have been assigned to the low-T, hydrothermal assemblage (Nixon et al., 1990). The general succession is as follows: (I) isoferroplatinum-II crystallized together with serpentine, chlorite, pentlandite and pyrrhotite, which is supported by the ubiquitous presence of these minerals in the outer parts of large isoferroplatinum grains (Fig. 9a-c, 11f) or in the serpentine veinlets (Fig. 9g-i); (II) tetraferroplatinum and tulameenite substitute isoferroplatinum (Fig. 9a-c, e); (III) tomamaeite and other Cu-rich minerals replace isoferroplatinum (Fig. 6f, 9e), ferronickelplatinum (Fig. 9h) and pentlandite (Fig. 9i), or occur as separate phases together with base-metal sulfides (Fig. 9k). The exact order of arsenide and sulfarsenide formation is unclear, but can be definitely assigned to be late stage, which is consistent with their

Table 2
Comparison of PGM assemblage of dunites, wehrlites and Matysken river placer.

Mineral	Dunite and chromitite	Wehrlite	Placer
Isoferroplatinum **Pt_3Fe** I generation	+++	–	+++
Isoferroplatinum II generation	+	–	+
Pd- and Sn-rich isoferroplatinum	–	+	–
Native osmium **Os**	+++	–	+++
Native iridium **Ir**	++	–	++
Tetraferroplatinum **PtFe**	+++	–	+++
Tulameenite **Pt_2FeCu**	++	–	++
Ferronickelplatinum **Pt_2FeNi**	+	–	+
Tomamaeite **Cu_3Pt**	+	–	–
Unnamed compound **Ni_2FePt**	+	–	–
Unnamed compound **Cu_4Pt**	++	–	–
Hexaferrum **(Fe,Os)**	+	–	–
Cooperite **PtS**	+	–	–
Laurite **RuS_2**	++	–	++
Erlichmanite **OsS_2**	++	–	+
Boweite **Rh_2S_3** – kashinite **Ir_2S_3**	+	–	–
Cuproiridsite **$CuIr_2S_4$**	++	–	–
Sperrylite **$PtAs_2$**	+	–	+
Irarsite **IrAsS**	++	–	–
Geversite **$PtSb_2$**	+	–	–
Unnamed compound **(Ir,Bi)(Te,Sb)**	+	–	–
Awaruite **Ni_3Fe***	++	–	+
Wairauite **CoFe***	+	–	–
Pentlandite **$(Fe,Ni)_9S_8$***	++	++	–
Pyrrhotite **Fe_7S_8***	+	+++	+
Sphalerite **ZnS**	+	+	–

Notes. "+"– mineral is rare, "++" mineral is widespread, "+++"– predominant mineral, "–"– not observed. * Base metal sulfides, awaruite and awaruite are given only if they are spatially related to PGM mineralization. For wehrlites the relation is an assumption only.

presence in serpentine veinlets in fractures in chromian spinel (Fig. 9f).

Another mineral which sheds light on the origin of the late stage PGM assemblage is awaruite. This mineral is common in ultramafic rocks, where it forms during serpentinization at a limited range of temperatures (~520°–350 °C and lower) under reduced conditions (Britten, 2017; Klein and Bach, 2009; Sciortino et al., 2015; Sidorov et al., 2018). Limited reports on the relationship between awaruite and PGM exist. Ahmed and Bevan (1981) reported Ir-bearing (up to 10 wt% Ir) awaruite coexisting with ruthenian hexaferrum in the Sakhakot-Qila ultramafics in Pakistan, and awaruite-PGM intergrowths were reported in the Galmoenan complex of the Ural-Alaskan type in the Koryak Highlands by Nazimova et al. (2011) and Sidorov et al. (2012). Zaccarini et al. (2016) recently reported Os-Ir-Ru alloys associated with awaruite and chlorite; Lawley et al. (2019) reported awaruite enriched in Pt and Pd relative to the parent pentlandite. In the Matysken complex, awaruite is associated with PGM (Fig. 9g-i, l) together with Cu-rich alloys, which form rims after pentlandite (Fig. 9g-i, l), similar to those between tulameenite and isoferroplatinum (Fig. 9e). This textural relationship presents direct evidence of crystallization of such alloys together with awaruite and restricts the range of conditions to low-temperature and reduced. The secondary mineral assemblage indicates that at least Pt, Ir and Rh were mobile during serpentinization. Reviews by Cabri and Aiglsperger (2018), Tolstykh et al. (2002b) show that minerals of Os (i.e. osarsite OsAsS) and Ru (various Ru-Fe-Os compounds) may also be present in the late assemblages of other Ural-Alaskan type complexes, but to a much lesser extent. González-Jiménez et al. (2015) proposed that the minute particles of Ru-Os-Ir alloys (<1 nm in diameter) were redistributed due to laurite desulphurization during hydrous metamorphism. Subsequently, these nanoparticles became unstable and coarsened to form larger (>1μm) particles. Another evidence of PGM alteration is provided by the study of ophiolites are Fe-Ru-Os-Ir oxides, resembling the hexaferrum composition in everything but oxygen content (e.g. Ahmed and Arai, 2003; Garuti et al., 1997b). The problem in the Matysken complex is that early-stage minerals of Ir, Rh, Os and Ru (alloys and laurite) do not show any signs of alteration, such as those observed for isoferroplatinum. Thus, the question at hand is: what was the source of Ir, Rh, Os and Ru essential for the formation of the late PGM assemblage? We suggest that these elements were extracted from isoferroplatinum during its alteration. The content of the impurities in newly formed tetraferroplatinum or tulameenite is significantly lower (commonly below detection limit) than in isoferroplatinum (Fig. 12b, c). Another possible explanation is that the alteration of BMS can theoretically provide significant amounts of PGE, because BMS may bear significant contents of several PGEs (e.g. Godel et al., 2007). However, the low BMS content in Matysken dunite renders this scenario to be unlikely.

7. Conclusions

1. Platinum mineralization in the Matysken complex is similar to those of other well-characterized Ural-Alaskan type complexes, including Galmoenan in the Koryak Highlands and complexes in the Ural Mountains. The PGM assemblage of the Matysken River placers indicates that the dunite unit of the complex is the only significant source of PGM for the placers. The long history of erosion and alluvium accumulation led to the mixing of material derived from various erosion levels and resulted in the broader compositional variations of placer PGMs compared with those of the lodes. Wehrlite bears insignificant Pt-Pd mineralization albeit in some samples shows the PGE content comparable to those of dunite, but does not make any significant contribution to the placer assemblage.
2. Platinum-group elements, with the exception of Pd, are quite uniformly distributed in dunite containing accessory chromian spinel and show good correlations between PGE and Cr. The calculated concentrations of Pt in accessory chromian spinel is of the same grade as for chromitites, thereby indicating that the formation of chromitites does not concentrate PGE over Cr, but only redistributes them into larger aggregates.
3. The Matysken complex dunite underwent two types of serpentinization: massive serpentinization in shear zones and marginal parts of the unit, and smaller scale serpentinization, which produced thin veinlets of serpentine in largely unaltered dunite. The former is barren, while the latter contains diverse mineralization, giving insights into the late stage crystallization/alteration of PGM. The serpentine-related PGM assemblages formed in the following order: (1) isoferroplatinum-II + pentlandite, (2) tetraferroplatinum + tulameenite, (3) tomamaeite and unnamed Cu-rich alloys + awaruite. These processes correspond with the progressive shift towards lower temperatures and more reduced conditions as a result of serpentinization.

Declaration of Competing Interest

The authors declare that they have no known competing financial interests or personal relationships that could have appeared to influence the work reported in this paper.

Acknowledgments

We are thankful to Alexey Razumny who provided unpublished results of 1995-2000 prospecting works, as well as all geologists who took part in the field trip to the Matysken complex during 2016-2017, especially Daria Bukhanova, Roman Novakov, Alexander Sorokin and German Evseev. Nadezhda Tolstykh is specially acknowledged for the internal review. Viktoria Danilovskaya is acknowledged for performing high-quality EPMA analyses. Editor in Chief Franco Pirajno and Associate Editor Olga Plotinskaya are largely acknowledged for their work. Authors are thankful to Reid Keays and anonymous reviewer for the constructive comments. This work was largely supported by the Russian Foundation for Basic Research (RFBR) grant No 20-05-00290 A.

Appendix A. Supplementary data

Supplementary data to this article can be found online at https://doi.org/10.1016/j.oregeorev.2020.103947.

References

Ahmed, A.H., Arai, S., 2003. Platinum-group minerals in podiform chromitites of the Oman ophiolite. Can. Mineral. 41, 597–616.

Ahmed, Z., Bevan, J.C., 1981. Awaruite, iridian awaruite, and a new Ru-Os-Ir-Ni-Fe alloy from the Sakhakot-Qila Complex, Malakand-Agency, Pakistan. Mineral. Mag. 44 (334), 225–230. https://doi.org/10.1180/minmag.1981.044.334.17.

Augé, T., Genna, A., Legendre, O., Ivanov, K.S., Volchenko, Y.A., 2005. Primary platinum mineralization in the Nizhny Tagil and Kachkanar ultramafic complexes, Urals, Russia: a genetic model for PGE concentration in chromite-rich zones. Econ. Geol. 100 (4), 707–732. https://doi.org/10.2113/gsecongeo.100.4.707.

Ballhaus, C., Berry, R.F., Green, D.H., 1991. High pressure experimental calibration of the olivine-orthopyroxene-spinel oxygen geobarometer: implications for the oxidation state of the upper mantle. Contrib. Miner. Petrol. 107, 27–40.

Barnes, S.J., Liu, W., 2012. Pt and Pd mobility in hydrothermal fluids: Evidence from komatiites and from thermodynamic modelling. Ore Geol. Rev. 44, 49–58.

Batanova, V.G., Astrakhantsev, O.V., 1992. Tectonic position and origins of the zoned mafic-ultramafic plutons in the Northern Olyutor Zone, Koryak Highlands. Geotectonics 26 (2), 153–165.

Batanova, V.G. and Astrakhantsev, O.V., 1994. Island arc mafic-ultramafic plutonic complexes of North Kamchatka. In: Proceedings of 29th International Geological Congress (January 1994), pp. 129–143.

Batanova, V.G., Astrakhantsev, O.V., Sidorov, E.G., 1991. The dunites of the Gal'moenansk pluton, Koryak Highlands. Int. Geol. Rev. 33 (1), 62–73. https://doi.org/10.1080/00206819109465672.

Batanova, V.G., Pertsev, A.N., Kamenetsky, V.S., Ariskin, A.A., Mochalov, A.G., Sobolev, A.V., 2005. Crustal evolution of island-arc ultramafic magma: Galmoenan pyroxenite-dunite plutonic complex, Koryak Highland (Far East Russia). J. Petrol. 46 (7), 1345–1366. https://doi.org/10.1093/petrology/egi018.

Betekhtin, A.G., 1954. Primary platinum depostis in Urals. In: AN SSSR, Moscow, pp. 22–57. [in Russian].

Britten, R., 2017. Regional metallogeny and genesis of a new deposit type-disseminated awaruite (Ni_3Fe) mineralization hosted in the cache creek terrane. Econ. Geol. 112 (3), 517–550. https://doi.org/10.2113/econgeo.112.3.517.

Bowles, J., Suárez, S., Prichard, H.M., Fisher, P.C., 2017. The mineralogy, geochemistry and genesis of the alluvial platinum-group minerals of the Freetown Layered Complex, Sierra Leone. Mineral. Mag.

Bowles, J.F.W., 1986. The development of platinum-group minerals in laterites. Econ. Geol. 81, 1278–1285.

Cabri, L.J., Feather, C.E., 1975. Platinum-iron alloys; a nomenclature based on a study of natural and synthetic alloys. Can. Mineral. 13 (2), 117–126.

Cabri, L.J., Harris, D.C., Weiser, T.W., 1996. Mineralogy and distribution of platinum-group mineral (PGM) placer deposits of the world. Explor. Min. Geol. 5 (2), 73–167.

Cabri, L.J., Aiglsperger, T., 2018. A review of hexaferrum based on new mineralogical data. Mineral. Mag. 1–16 https://doi.org/10.1180/mgm.2018.86.2.

Cui, M.-M., Su, B.-X., Wang, J., Chen, K.-Y., Sakyi, P.A., Tang, D.-M., He, Y.-P., Sun, J.-G., Cui, J., Anani, C.Y., Gao, D.-L., 2020. Alaskan-type nature and PGE mineralization of the Wuxing mafic–ultramafic complex in eastern part of the Central Asian Orogenic belt. Ore Geol. Rev. 123.

Garuti, G., Fershtater, G., Bea, F., Montero, P., Pushkarev, E.V., Zaccarini, F., 1997a. Platinum-group elements as petrological indicators in mafic-ultramafic complexes of the central and southern Urals: preliminary results. Tectonophysics 276 (1–4), 181–194. https://doi.org/10.1016/S0040-1951(97)00050-4.

Garuti, G., Zaccarini, F., Cabella, R., Ferstater, G., 1997b. Occurrence of unknown Ru-Os-Ir-Fe oxides in the chromitites of the Nurali ultramafic complex, Southern Urals, Russia. Can. Mineral. 35, 1431–1439.

Godel, B., Barnes, S.J., Maier, W.D., 2007. Platinum-group elements in sulphide minerals, platinum-group minerals, and whole-rocks of the Merensky Reef (Bushveld Complex, South Africa): Implications for the formation of the reef. J. Petrol. 48 (8), 1569–1604. https://doi.org/10.1093/petrology/egm030.

González-Jiménez, J.M., Gervilla, F., Kerestedjian, T., Proenza, J.A., 2010. Alteration of platinum-group and base-metal mineral assemblages in ophiolite chromitites from the Dobromirtsi massif, Rhodope Mountains (Bulgaria). Resour. Geol. 60 (4), 315–334.

González-Jiménez, J.M., Reich, M., Camprubí, A., Gervilla, F., Griffin, W.L., Colás, V., O'Reilly, S.Y., Proenza, J.A., Pearson, N.J., Centeno-García, E., 2015. Thermal metamorphism of mantle chromites and the stability of noble-metal nanoparticles. Contrib. Miner. Petrol. 170 (2).

Hanley, J.J., 2005. The aqueous geochemistry of the platinum-group elements (PGE) in surficial, low-T hydrothermal and high-T magmatic-hydrothermal environments. Explor. Platinum-group element deposits 35, 35–56.

Harris, D.C., Cabri, L.J., 1991. Nomenclature of platinum-group-element alloys: Review and revision. Can. Mineral. 29, 231–237.

Ivanov, O.K., 1997. Concentrically-zoned pyroxenite-dunite massifs of Urals. Urals State University Press, Yekaterinburg, pp. 487–487 pp. (in Russian).

Johan, Z., 2002. Alaskan-type complexes and their platinum-group element mineralization. In: Cabri, L.J. (Ed.), The geology, geochemistry, mineralogy and mineral beneficiation of platinum-group elements. Canadian Institute of Mining, Metallurgy and Petroleum, pp. 669–719.

Kepezhinskas, P.K., Taylor, R.N., Tanaka, H., 1993. Geochemistry of plutonic spinels from the North Kamchatka Ark: comparisons with spinels from other tectonic settings. Mineral. Mag. 57, 575–589.

Klein, F., Bach, W., 2009. Fe-Ni-Co-O-S Phase Relations in Peridotite-Seawater Interactions. J. Petrol. 50 (1), 37–59.

Konstantinovskaia, E.A., 2001. Arc-continent collision and subduction reversal in the Cenozoic evolution of the Nortwest Pacific: An example from Kamchatka (NE Russia). Tectonophysics 333 (1–2), 75–94. https://doi.org/10.1016/S0040-1951(00)00268-7.

Konstantinovskaya, E., 2011. Early Eocene Arc – Continent collision in Kamchatka, Russia: structural evolution and geodynamic model. In: Brown, D., Ryan, P.D. (Eds.), Arc-continent collision. Springer-Verlag, Berlin Heidelberg, Frontiers in Earth Sciences.

Kozlov, A.P., Chanturiya, V.A., Sidorov, E.G., Tolstykh, N.D. and Telegin, Y.M., 2011. Large-volume platinum ore deposits in zonal mafic-ultramafic complexes of the Ural-Alaskan type and the outlook for their development. Geol. Ore Deposits 53(5), 374–374. 10.1134/s1075701511050059.

Krause, J., Brügmann, G.E., Pushkarev, E.V., 2007. Accessory and rock forming minerals monitoring the evolution of zoned mafic-ultramafic complexes in the Central Ural Mountains. Lithos 95 (1–2), 19–42. https://doi.org/10.1016/j.lithos.2006.07.018.

Kutyev, F.S., Sidorov, E.G., Reznichenko, V.S., Semyonov, V.L., 1991. New data about platinoids in zoned ultrabasic complexes of the Southern part of Koryak Highland. Dokl. Akad. Nauk USSR 317, 1458–1461 [in Russian].

Kutyrev, A.V., Kamenetsky, V.S., Sidorov, E.G., Abersteiner, A. and Chubarov, V.M., 2020. Silicate inclusions in isoferroplatinum: Constraints on the origin of platinum mineralization in podiform chromitites. Ore Geol. Rev. 119(October 2019). 10.1016/j.oregeorev.2020.103367.

Kutyrev, A.V., Sidorov, E.G., Antonov, A.V., Chubarov, V.M., 2018. Platinum-group mineral assemblage of the Prizhimny Creek (Koryak Highland). Russ. Geol. Geophys. 59 (8), 935–944. https://doi.org/10.1016/j.rgg.2018.07.014.

Kutyrev, A.V., Zhirnova, T.S., 2019. Concentrically-zoned massifs of the Tamanvayam group (Koryak–Kamchatka Platiniferous Belt): structure, age, petrological and geochemical aspects. Russ. J. Pac. Geol. 13 (4), 350–363. https://doi.org/10.1134/S1819714019040031.

Lawley, C.J.M., Petts, D.C., Jackson, S.E., Zagorevski, A., Pearson, D.G., Kjarsgaard, B.A., Savard, D., Tschirhart, V., 2019. Precious metal mobility during serpentinization and breakdown of base metal sulphide. Lithos 354–355 (xxxx), 105278. https://doi.org/10.1016/j.lithos.2019.105278.

Ledneva, G.V., Soloviev, A.V., Garver, J.I., 2000. Massifs of the heterogeneous mafic-ultramafic complex of the Olyutorsky zone, Koryak Mountains: Petrology and geodynamic aspects. Petrology 8 (5), 428–454 [in Russian].

Li, C., Ripley, E.M., Thakurta, J., Stifter, E.C., Qi, L., 2013. Variations of olivine Fo-Ni contents and highly chalcophile element abundances in arc ultramafic cumulates, southern Alaska. Chem. Geol. 351, 15–28. https://doi.org/10.1016/j.chemgeo.2013.05.007.

Loewinson-Lessing, F., 1900. Geological essay on Yuzhno-Zaozarskaya Dacha and Denezhkin Kamen complexes in Northern Urals. Trudy Imperatorskogo Obschestva Estestvoispytateley 30, 1–257 [in Russian].

Lyubetskaya, T., Korenaga, J., 2007. Chemical composition of Earth's primitive mantle and its variance: 1. Method and results. Journal of Geophysical Research: Solid. Earth 112 (3), 1–21. https://doi.org/10.1029/2005JB004223.

Mertie, J.B., Jr., 1969. Economic Geology of the Platinum Group metal. USGS, pp. 119–119.

Malitch, K.N., Thalhammer, O.A.R., 2002. Pt–Fe nuggets derived from clinopyroxenite–dunite massifs, Russia: a structural, compositional and osmium-Isotope study. Can. Mineral. 40 (2), 395–418.

Mochalov, A.G., 2013. A genetic model of PGM hosted in cumulative gabbro-pyroxenite-dunite complexes of the Koryak Highland, Russia. Geol. Ore Deposits 55 (3), 145–161. https://doi.org/10.1134/s1075701513030033.

Mochalov, A.G., Dmitrenko, G.G., Rudashevsky, N.S., Zhernovsky, I.V., Boldyreva, M.M., 1998. Hexaferrum (Fe, Ru), (Fe, Os), (Fe, Ir) – a new mineral. Proc. Russ. Mineral. Soc. 127 (5), 41–51 [in Russian].

Murray, C.G., 1972. Zoned ultramafic complexes of the alaskan type: feeder pipes of andesitic volcanoes. Geol. Soc. Am. Mem. 132 (1967), 313–336.

Nazimova, Y.V., Zaytsev, V.P., Petrov, S.V., 2011. The Galmoenan massif, Kamchatka, Russia: geology, PGE mineralization, applied mineralogy and beneficiation. Can. Mineral. 49 (6), 1433–1453. https://doi.org/10.3749/canmin.49.6.1433.

Nekrasov, I.Y., Lennikov, A.M., Oktyabrysky, R.A., Zalischak, B.L., Sapin, V.I., 1994. Petrology and platinum potential of annular alkaline complexes. Nauka, Moscow, p. 381.

Nixon, G.T., Cabri, L.J., Laflame, G.J.H., 1990. Platinum-group-element mineralization in lode and placer deposits associated with the Tulameen Alaskan-type comples, British Columbia. Can. Mineral. 28 (May), 503–535.

Oberthür, T., Melcher, F., Fusswinkel, T., van den Kerkhof, A.M., Sosa, G.M., 2018. The hydrothermal Waterberg platinum deposit, Mookgophong (Naboomspruit), South Africa. Part 1: Geochemistry and ore mineralogy. Mineral. Mag. 82 (3), 725–749.

O'Driscoll, B., González-Jiménez, J.M., 2016. Petrogenesis of the platinum-group minerals. Rev. Mineral. Geochem. 81 (1), 489–578. https://doi.org/10.2138/rmg.2016.81.09.

Okrugin, A.V., 2011. Origin of platinum-group minerals from dispersed elements to nuggets in mafic-ultramafic intrusive rocks. Can. Mineral. 49, 1397–1412. https://doi.org/10.3749/canmin.49.6.1397.

Palamarchuk, R.S., Stepanov, S.Y., Khanin, D.A., Antonov, A.V., 2017. PGE mineralization of massive chromitites of the Iov Dunite body (Northern Urals). Mosc. Univ. Geol. Bull. 72 (6), 445–454. https://doi.org/10.3103/S0145875217060096.

Pushkarev, E.V., Anikina, E.V., Garuti, G., Zaccarini, F., 2007. Chromium-platinum deposits of Nizhny-Tagil type in the Urals: structural-substantial characteristic and a problem of genesys. Litosfera 92 (3), 28–65 [in Russian].

Pushkarev, E.V., Kamenetsky, V.S., Morozova, A.V., Khiller, V.V., Glavatskykh, S.P., Rodemann, T., 2015. Ontogeny of ore Cr-spinel and composition of inclusions as indicators of the pneumatolytic–hydrothermal origin of PGM-bearing chromitites from Kondyor massif, the Aldan Shield. Geol. Ore Deposits 57 (5), 352–380. https://doi.org/10.1134/s1075701515050049.

Qin, K., Guo, Z., Tang, D., Li, J., Guo, X., Dong, L., 2018. Discovery of Alaskan-style Tuerkubantao maficultramafic complex in NW-Junggar, NW China, and its significance. Yanshi Xuebao/Acta Petrol. Sin. 34 (7), 1897–1913.

Razin, L.V., 1976. Geologic and genetic features of forsterite dunites and their platinum-group mineralization. Econ. Geol. 71, 1371–1376. https://doi.org/10.2113/gsecongeo.71.7.1371.

Scholten, L., Watenphul, A., Beermann, O., Testemale, D., Ames, D., Schmidt, C., 2018. Nickel and platinum in high-temperature H2O + HCl fluids: Implications for hydrothermal mobilization. Geochim. Cosmochim. Acta 224, 187–199.

Sciortino, M., Mungall, J.E., Muinonen, J., 2015. Generation of High-Ni sulfide and alloy phases during serpentinization of dunite in the Dumont Sill, Quebec. Econ. Geol. 110 (3), 733–761. https://doi.org/10.2113/econgeo.110.3.733.

Shapiro, M.N., Soloviev, A.V., 2009. Formation of the Olyutorsky-Kamchatka foldbelt: a kinematic model. Russ. Geol. Geophys. 50 (8), 668–681. https://doi.org/10.1016/j.rgg.2008.10.006.

Sidorov, E.G., Kozlov, A.P., Tolstykh, N.D., 2012. The Galmoenan ultrabasic massif and its platinum potential. Nauchnyi Mir, Moscow, 288 pp. [in Russian].

Sidorov, E.G., Kutyrev, A.V., Zhitova, E.S., Chubarov, V.M., Khanin, D.A., 2019. Origin of platinum-group mineral assemblages from placers in rivers draining from the Ural-Alaskan type Itchayvayamsky ultramafics, Far East Russia. Can. Mineral. 57 (1), 91–104. https://doi.org/10.3749/canmin.1800040.

Sidorov, E.G., Sandimirova, E.I., Chubarov, V.M., Ananiev, V.V., 2018. Accessory minerals of the mafic-ultramafic massif Galmoenan (Koryakskoye upland, Kamchatka). Proc. Russ. Mineral. Soc. 147 (2), 44–64. https://doi.org/10.30695/zrmo/2018.1472.03.

Stepanov, S.Y., Malitch, K.N., Kozlov, A.V., Badanina, I.Y., Antonov, A.V., 2017. Platinum group element mineralization of the Svetly Bor and Veresovy Bor clinopyroxenite–dunite massifs, Middle Urals, Russia. Geol. Ore Deposits 59 (3), 244–255. https://doi.org/10.1134/s1075701517030060.

Stepanov, S.Y., Palamarchuk, R.S., Antonov, A.V., Kozlov, A.V., Valrlamov, D.A., Khanin, D.A., Zolotarev Jr, A.A., 2020. Morphology, composition, and ontogenesis of platinum-group minerals in chromitites of zoned clinopyroxenite-dunite massifs the Middle Urals. Russ. Geol. Geophys. 61(1), 47–67. 10.15372/rgg2019089.

Tarkian, M., Stribrny, B., 1999. Platinum-group elements in porphyry copper deposits: a reconnaissance study. Mineral. Petrol. 65, 161–183.

Taylor, H.P.J., 1967. The zoned ultramafic complexes of southeastern Alaska. In: Wyllie, P.J. (Ed.), Ultramafic and related rocks. John Wiley, New York, pp. 98–118.

Thakurta, J., 2018. Alaskan-type complexes and their associations with economic mineral deposits. Elsevier Inc., pp. 269–302

Tolstykh, N., Kozlov, A. and Telegin, Y., 2015. Platinum mineralization of the Svetly Bor and Nizhny Tagil intrusions, Ural Platinum Belt. Ore Geol. Rev. 67, 234–243.https://doi.org/10.1016/j.oregeorev.2014.12.005.

Tolstykh, N., Krivenko, A., Sidorov, E., Laajoki, K. and Podlipsky, M., 2002a. Ore mineralogy of PGM placers in Siberia and the Russian Far East. Ore Geol. Rev. 20(1), 1–25.https://doi.org/10.1016/S0169-1368(02)00036-7.

Tolstykh, N.D., Foley, J.Y., Sidorov, E.G., Laajoki, K.V.O., 2002b. Composition of the platinum-group minerals in the Salmon river placer deposit, goodnews bay. Alaska 463–471.

Tolstykh, N.D., Sidorov, E.G., Kozlov, A.P., 2004. Platinum-group minerals in lode and placer deposts associated with the Ural-Alaskan-type Gal'moenan complex, Koryak-Kamchatka Platinum Belt, Russia. Can. Mineral. 42 (2), 619–630.

Tolstykh, N.D., Sidorov, E.G., Laajoki, K.V.O., Krivenko, A.P., Podlipsky, M., 2000. The association of platinum-group minerals in placers of the Pustaya River, Kamchatka, Russia. Can. Mineral. 38 (5), 1251–1264. https://doi.org/10.2113/gscanmin.38.5.1251.

Vildanova, E.Y., Zaytsev, V.P., Kravchenko, L.I., Landa, E.A., Litvinenko, A.F., Markovsky, B.A., Melkomukov, V.N., Mochalov, A.G., Nazimova, Y.V., Popruzhenko, S.V., Razumny, A.V., 2002. Koryak-Kamchatka region - New platiniferous province of Russia. VSEGEI, Saint-Petersburg, pp. 386–386 [in Russian].

Vysotsky, N.V., 1913. Platinum deposits of Isovsky and Nizhny Tagil districts of Ural. Trudy Geologicheskogo Komiteta 62, 1–693 [in Russian].

Zaccarini, F., Pushkarev, E., Garuti, G. and Kazakov, I., 2016. Platinum-Group Minerals and Other Accessory Phases in Chromite Deposits of the Alapaevsk Ophiolite, Central Urals, Russia. Minerals, 6(4), 108-108.10.3390/min6040108.

Zhu, Q., Zhu, Y., 2019. Platinum-group minerals and Fe–Ni minerals in the Sartohay podiform chromitite (west Junggar, China): Implications for T–pH–fO2–fS2 conditions during hydrothermal alteration. Ore Geol. Rev. 112(March 2018), 103020-103020.10.1016/j.oregeorev.2019.103020.

Zinkevich, V.P., Tsukanov, N.V., 1992. The formation of the accretional structure of eastern Kamchatka in the Late Mesozoic and early Cenozoic. Geotectonics 26, 332–343.